Accurate Intermolecular Potentials Obtained from Molecular Wave Functions: Bridging the Gap between Quantum Chemistry and Molecular Simulations

Ola Engkvist

J. Heyrovský Institute of Physical Chemistry, Academy of Sciences of the Czech Republic, Dolejškova 3, 182 23 Prague 8, Czech Republic

Per-Olof Åstrand

Condensed Matter Physics and Chemistry Department, Risø National Laboratory, P.O.B 49, DK-4000 Roskilde, Denmark

Gunnar Karlström*

Department of Theoretical Chemistry, Chemical Centre, University of Lund, P.O.B. 124, S-221 00 Lund, Sweden

Received January 4, 2000

Contents

1. Introduction

The forces between molecules govern the properties of condensed phases consisting of molecular entities. It is therefore of fundamental importance in science to understand the origin of intermolecular interactions and to be able to calculate the magnitude of these forces.[1,2] It is trivial, in principle, to calculate intermolecular interaction energies by regular quantum chemical methods. The interaction energy, E_{int}, for two molecules is simply given as the difference between the total energy of the complex, E_{AB}, and the monomer energies, E_{A} and E_{B}, as

$$E_{\mathrm{int}} = E_{\mathrm{AB}} - E_{\mathrm{A}} - E_{\mathrm{B}} \tag{1}$$

which theoretically can be calculated to any accuracy. The main disadvantage is that sophisticated quantum chemical calculations of even just a few molecules quickly become exceedingly demanding in terms of computer power. On the other hand, in studies of liquids and solutions, the interaction energy is normally calculated from interaction parameters, for example as in a site−site Lennard−Jones-type of potential

$$E_{\mathrm{int}} = \sum_{i,j} \frac{q_i q_j}{R_{ij}} + \frac{a_{ij}}{R_{ij}^{12}} - \frac{c_{ij}}{R_{ij}^{6}} \tag{2}$$

where the R^{-1} term describes the electrostatic interactions, the R^{-12} term models the short-range repulsion energy, and the R^{-6} term gives the dispersion energy. The advantage of this form is that it is computationally efficient and can be carried out for a system of many molecules, although obviously the accuracy is less than that obtained from quantum chemical calculations. Furthermore, the partitioning of the interaction energy by this form into different contributions, each with a physical meaning, gives insight into the nature of the interactions.

The goal of this review is to discuss how parameters for calculating intermolecular interactions can

* To whom correspondence should be addressed. Phone: +46 46 222 82 48. Fax: +46 46 222 45 43. E-mail: gunnar.karlstrom@teokem.lu.se.

10.1021/cr9900477 CCC: $35.00
Published on Web 10/24/2000

Ola Engkvist finished his Ph.D. degree in 1997 at the Department of Theoretical Chemistry, University of Lund, Sweden, with Professor Gunnar Karlström as his supervisor. Thereafter he spent six months in the laboratory of Professor Hobza, J. Heyrovský Institute of Physical Chemistry, Czech Academy of Sciences, Prague. Then he obtained a Marie Curie postdoctoral fellowship to work with Dr. Stone, University Chemical Laboratory, University of Cambridge. Dr. Engkvist is presently back in Dr. Hobza's group working on intermolecular interactions in DNA. His main research interests are intermolecular interactions in various systems of chemical importance, such as clusters, adsorption on surfaces, crystallization, and biochemical systems.

Per-Olof Åstrand was born in 1965 in Sätila, Sweden. He received his M.Sc. degree in Chemical Engineering in 1990, his Ph.D. degree in Theoretical Chemistry in 1995, and his docent degree in 1999, all from the University of Lund. His thesis research was carried out on intermolecular interactions with Dr. Gunnar Karlström as his thesis supervisor. In 1995, he joined the group of Dr. Kurt V. Mikkelsen at the University of Aarhus and from 1996 at the University of Copenhagen. Since 1998 he has been a Research Scientist at Risö National Laboratory, Roskilde. His research interests are in optical and magnetic properties of molecules, vibrational dynamics, solvent effects on molecular properties, intermolecular interactions, and simulations of liquids and solutions.

Gunnar Karlström completed his Master of Science degree in Chemical Engineering at the Technical Faculty, University of Lund, Lund, Sweden, in 1972. In 1978 he completed his thesis under the supervision of Professor Sture Forsen. Since then he has been working at the Departments of Physical Chemistry 2 and Physical Chemistry 1 and is presently a Professor at the Department of Theoretical Chemistry at the University of Lund. Professor Karlström's main research interests are intermolecular interactions and the link between the quantum and statistic mechanical worlds.

be obtained from molecular wave functions. The theoretical basis of this method is to regard the intermolecular interaction as a perturbation to the molecular wave functions.[1,3−9] In particular, at the long-range limit, the interaction energy may be obtained from molecular properties in a form that is consistent with classical electrostatics and to some extent resembles eq 2.[1,3,10] Furthermore, the goal of this method is to use the constructed intermolecular potentials in large-scale simulations of liquids and solutions. In a molecular dynamics (MD) or Monte Carlo (MC) simulation, the interactions have to be calculated repeatedly (10^5-10^8 times) for a large number of molecules, and thus, the calculation of the intermolecular forces is the most time-consuming part of these kinds of simulations.[11,12] Obtaining an intermolecular potential suitable for simulations of liquids thus has to be a compromise between accuracy and computational efficiency. A method termed NEMO has been developed along these lines and employed in studies of clusters and solutions.[13−17]

Accurate quantum chemical calculations of intermolecular interactions have been discussed by Hobza[18,19] among others, and potentials suitable for simulations have been obtained from supermolecular quantum chemical calculations.[20−28] Supermolecular DFT calculations usually describe hydrogen-bonded systems reasonably well.[29] However, DFT usually fails completely for complexes bounded by dispersive interactions.[19]

Empirical potentials are overwhelmingly used in existing molecular simulation packages.[30−33] These simulations have revealed a lot of interesting structural and dynamical data for different molecular systems, although severe criticism against these simulations also has been raised.[34] The empirical potentials usually are constructed to reproduce experimental data such as solvation energies, structural data obtained from crystals, observed radial distribution functions in the liquid, thermodynamic data, and to some extent quantum chemical calculations. The accuracy of calculations employing these potentials therefore is expected to be good for simulations performed on environments close to the ones for which the potential parameters were fitted. Semiempirical potentials also may be constructed by obtaining the electrostatics from the molecular wave function and the dispersion and repulsion parameters from empirical parameters, as illustrated by the work of Dykstra and co-workers.[35−38]

Quantum chemical methods also allow the calculation of intermolecular forces for the entire system at each step of the simulation. At present, this type of calculation is performed using a plane-wave basis set DFT model in MD simulations,[39] according to the so-called Car−Parrinello (CP) method. The calculations

are very time-consuming, so thus far only small systems have been studied over short periods. However, the method has been successfully used to study, for example, liquid water[40,41] and hydrated protons in water.[42] In general, CP MD is a useful method, especially for studying systems where covalent bonds are broken and formed.

Many intermolecular potentials have been constructed to study various forms of hydrogen bonding. The study of hydrogen-bonding interactions is of particular interest for many reasons.[43] Hydrogen bonds arise between polar groups of molecules (or within molecules) and are dominated by electrostatic interactions. The large electric fields which arise from the polarity of the molecules also lead to large polarization contributions, and these are most conveniently modeled by explicit polarizabilities that take into account the inhomogeneity of the electronic structure of the surroundings. Electrostatic interactions have been discussed in more detail than repulsion and dispersion interactions,[38,44] and polarizable models have been applied to the electrostatics in large biomolecular simulations.[45,46] It has been demonstrated that hydrogen bonds are extremely orientation-dependent,[47,48] and thus, they cannot be modeled adequately by spherically symmetric atomic charges. In water, for example, the atomic charges only can reproduce the molecular dipole moment. However, water has a tetrahedral structure in liquid water (as well as in ice) leading to a very small dipole−dipole interaction energy by symmetry arguments.[49] Thus dipole−quadrupole and quadrupole−quadrupole interactions are important, and an accurate description of the molecular quadrupole moment of water is required.

This review discusses intermolecular potentials which are obtained from molecular wave functions and are suitable for simulations. Some background theory is given, and applications to molecular clusters, interactions at surfaces, liquids and solutions, flexible molecules in solution, and solvent effects on molecular properties are discussed. The review is focused on applications done in the past decade.

2. Theory

Ab initio quantum chemical calculations have contributed to our understanding of chemical phenomena in many ways. Perhaps it is within the field of intermolecular interactions that quantum chemical methods have most significantly increased our understanding of the mechanisms governing the behavior of molecular systems. Two different approaches have been used to study intermolecular interactions: the perturbation approach and the supermolecular approach. The perturbation approach treats the interaction between the monomer wave functions as a perturbation and the interaction energy is evaluated using perturbation theory.[1,7,8,50−52] The most successful perturbation theory for intermolecular interactions is the symmetry-adapted perturbation theory (SAPT) by Jeziorski et al.[7] The intermolecular perturbation theory (IMPT)[53] developed by Stone et al. is a special case of the SAPT. Alternatively, in the supermolecular approach, the interaction energy is calculated as the difference between the energy of the dimer complex and the energy of the monomers.[18,19] Since the interaction energy is only a very small part of the total energy, these supermolecule calculations have to be of high quality. The connection between the supermolecular approach and the perturbation approach has been recently discussed in *Chemical Reviews*.[54]

High-quality supermolecular calculations result in the best estimates of interaction energies that are available today, and they can be used to calibrate and establish the reliability of other methods. The perturbation method, on the other hand, can be used to construct accurate intermolecular potentials, and these potentials can then be used to study clusters and bulk liquids. We will begin the theory section by briefly discussing the application of perturbation theory to intermolecular interactions. We will then give a description of how to construct intermolecular potentials using a perturbation approach. It should be emphasized that although the constructed intermolecular potentials are based on perturbation theory, supermolecular calculations are needed to calibrate and test the constructed potentials. A more detailed presentation of the theory of intermolecular interactions can be found in the recent book by Stone.[8]

2.1. RS Perturbation Theory for Intermolecular Interactions at Long Ranges

Regular Rayleigh−Schrödinger (RS) perturbation theory in the long-range limit[1,4,8] provides a good starting point for the evaluation of intermolecular interaction energies when it is assumed that exchange effects are not included, i.e., the Pauli principle is not imposed between the molecules. This assumption is usually called the polarization approximation, and its deficiencies have been discussed.[55−58] We will denote the Hamiltonian for molecule 1 as $\hat{H}^1$ and for molecule 2 as $\hat{H}^2$. The ground-state wave functions are denoted by ψ_0^1 and ψ_0^2, and the wave functions for the excited states are denoted by ψ_a^1 and ψ_b^2. The corresponding eigenvalues (energies) are denoted as ϵ_0^1, ϵ_0^2, ϵ_a^1, and ϵ_b^2, respectively. The intermolecular interaction part of the Hamiltonian is defined as the difference between the total Hamiltonian for the system and the Hamiltonians for the monomers

$$\hat{V} = \hat{H} - \hat{H}^1 - \hat{H}^2 \tag{3}$$

The explicit expression for V (in atomic units) is

$$\hat{V} = \sum_{K_1}\sum_{L_2}\frac{Z_K Z_L}{r_{KL}} - \sum_{K_1}\sum_{j_2}\frac{Z_K}{r_{KL}} - \sum_{i_1}\sum_{L_2}\frac{Z_L}{r_{Li}} + \sum_{i_1}\sum_{j_2}\frac{1}{r_{ji}} \tag{4}$$

where K and L are nuclei and Z_K and Z_L are their corresponding charges.

By regarding $\hat{V}$ as the perturbation operator and applying the RS perturbation method to the ground-state wave function of $(\hat{H}^1 + \hat{H}^2)$, which is the direct product $\psi_0{}^1\psi_0{}^2$, the following expansion is obtained

for the perturbation energy when truncated after the second-order terms

$$\Delta E^{\mathrm{RS}} = \langle \psi_0^1 \psi_0^2 | \hat{V} | \psi_0^1 \psi_0^2 \rangle \text{ (electrostatic term)}$$

$$- \sum_{a>0} \frac{|\langle \psi_0^1 \psi_0^2 | \hat{V} | \psi_a^1 \psi_0^2 \rangle|^2}{\epsilon_a^1 - \epsilon_0^1} \text{ (Polarization of 1 by 2)}$$

$$- \sum_{b>0} \frac{|\langle \psi_0^1 \psi_0^2 | \hat{V} | \psi_0^1 \psi_b^2 \rangle|^2}{\epsilon_b^2 - \epsilon_0^2} \text{ (Polarization of 2 by 1)}$$

$$- \sum_{a>0} \sum_{b>0} \frac{|\langle \psi_0^1 \psi_0^2 | \hat{V} | \psi_a^1 \psi_b^2 \rangle|^2}{\epsilon_a^1 + \epsilon_b^2 - \epsilon_0^1 - \epsilon_0^2} \text{ (dispersion term)} \quad (5)$$

The electrostatic term is a first-order term, while the others are second-order terms. The Rayleigh−Schrödinger perturbation approach to intermolecular interactions neglects the exchange of the molecular charge distributions at the long-range limit. However, more sophisticated approaches such as symmetry-adapted perturbation theory (SAPT)[7,59] and intermolecular perturbation theory (IMPT)[8,60] exist which include the exchange terms in the perturbation expansion. The perturbation expansion in eq 5 is only valid at long-range separation of the molecules, since the total wave function is not antisymmetric with respect to the interchange of electrons between molecule 1 and 2. If the total wave function is antisymmetrized, first-order and higher exchange−repulsion terms will also appear.[7]

2.2. Intermolecular Interactions with a Perturbation Approach

In this section, we will outline the theory and details of perturbation approaches aimed at describing intermolecular interactions. The fundamental idea behind these approaches is to use information about the molecular charge and polarizability distribution which is obtained from ab initio calculations on the isolated molecules. Several schemes have been developed to construct accurate intermolecular potentials in this manner, primarily using information that can be obtained from the monomer wave functions.[13,14,61−66] A difference between the approaches occurs in the way the functional form of the potential is simplified. A complex functional form would be best in that it would allow a more accurate description of the potential. However, the computational cost of this complexity is high and may become too large for bulk simulations.

The first step is to carry out a so-called multipole expansion of the molecular charge distributions.[67] The electronic part of the operator $\hat{V}$ can be written as

$$\hat{V}^{ee} = \sum_{i^1} \sum_{j^2} \frac{1}{r_{ji}} \sum_{i^1} \sum_{j^2} \frac{1}{|\vec{r}_i - \vec{r}_j + \vec{R}|} \quad (6)$$

where $\vec{R}$ is the distance between the centers of mass of molecules 1 and 2 and $\vec{r}_i$ is the distance between electron i and the center of mass for molecule 1. If it is assumed that both $\vec{r}_i$ and $\vec{r}_j$ are much smaller than $|\vec{R}|$, $\hat{V}^{ee}$ can be expanded in a multipole series around the center of mass of the molecules

$$\hat{V}^{ee} = \frac{1}{R} + \sum_i r_{i\alpha} \nabla_\alpha \left(\frac{1}{R}\right) - \sum_j r_{i\alpha} \nabla_\alpha \left(\frac{1}{R}\right) + \ldots \quad (7)$$

Here and in the remainder of this review the Einstein summation convention is used for summation over repeated indices. When the multipole expansion is combined with the assumption that the total wave function can be modeled by the direct product $\psi_0^1 \psi_0^2$, the intermolecular interactions can be calculated solely from the properties of the individual molecules and a function describing the intermolecular distance and orientation.

One drawback to this approach is that a multipole expansion does not converge for intermolecular distances shorter than the intramolecular distances. This problem can be resolved by carrying out the multipole expansion at several points within each molecule, for example at the atomic positions. However, the partitioning of molecular properties into atomic contributions is nontrivial, primarily because atomic properties are not measurable quantities. Thus, there is an inherent ambiguity as to how atomic properties should be defined, and as a consequence, numerous ways exist to calculate properties such as atomic charges and polarizabilities. A scheme for partitioning a molecular property into atomic properties should fulfill some fundamental conditions:[68] proper additivity ($\sum_{i=1}^{N} \Omega_i = \Omega$), invariance with respect to the choice of origin, and the same transformation properties for molecular and the corresponding atomic properties with respect to characteristics such as a rotation of the molecule. Another desired feature is that the atomic contributions closely model higher-order molecular properties. For example, a model for atomic charges should give an accurate molecular dipole moment and a reasonable molecular quadrupole moment and a model for atomic polarizabilities should result in reasonable molecular higher rank polarizabilities.

The intermolecular interaction energy is usually divided into four contributions

$$E^{\mathrm{tot}} = E^{\mathrm{ele}} + E^{\mathrm{ind}} + E^{\mathrm{ere}} + E^{\mathrm{disp}} \quad (8)$$

where E^{ele} is the electrostatic energy, E^{ind} the induction energy, E^{ere} the exchange−repulsion energy, and E^{disp} the dispersion energy.

The exchange−repulsion energy term may be approximated as being proportional to the overlap of the wave functions[4] and usually is modeled as either an isotropic or anisotropic exponentially decaying function. The dispersion term is often modeled using a modified (damped) London-type expression.[67] Fi-

nally, an explicit term describing charge-transfer contributions can be added to the potential.[69]

2.2.1. The Electrostatic Energy

Assuming that overlap effects may be neglected, the electrostatic energy can be calculated as the interaction between the multicenter multipole expansions extracted from the wave function for the monomers. Local electrostatic moments are not observables; therefore, they can be calculated in different ways.[70−83] Electrostatic models have already been extensively reviewed;[38,44] thus, a general description of all the different models will not be given here.

In some of the methods,[70,72,77] it is used that the molecular orbitals, ϕ_i, are constructed from a set of basis functions, χ_μ

$$\psi_i = \sum_\mu c_{i\mu}\chi_\mu \tag{9}$$

where $c_{i\mu}$ is an orbital coefficient. The density matrix D is defined as

$$D_{\mu\nu} = \sum_i n_i c_{i\mu} c_{i\nu} \tag{10}$$

where n_i is the occupation number for orbital i. Accordingly, the total molecular charge can be written as

$$\rho = \sum_\mu \sum_\nu D_{\mu\nu}\chi_\mu\chi_\nu \tag{11}$$

The charge distribution can be divided into local contributions $\tilde{n}_{KL}$, where K and L are nuclei, since each basis function may be assigned to a nucleus

$$\rho_{KL} = \sum_{\mu\in K} \sum_{\nu\in L} D_{\mu\nu}\chi_\mu\chi_\nu \tag{12}$$

A local charge for each atom pair is calculated as

$$q_{KL} = \sum_{\mu\in K} \sum_{\nu\in L} D_{\mu\nu}\langle\chi_\mu|\chi_\nu\rangle \tag{13}$$

The nuclear charges are most conveniently added to the diagonal charges q_{KK}. If Gaussian basis functions are adopted, the overlap integral over two basis functions, $\langle\chi_\mu|\chi_\nu\rangle$, is given in terms of a single Gaussian function with an expansion point between the two nuclei. For each pair of basis functions, the contribution to q_{KL} ($K \neq L$) is regarded as a point charge situated between the two nuclei. These point charges are normally moved to reduce the number of expansion points and it is here where the various approaches differ. In the original Mulliken approach, one-half of the contribution is moved to each nucleus.[84]

Local dipole moments, quadrupole moments, and higher-order moments can be calculated in an equivalent manner by exchanging the overlap integral in eq 13 with the dipole integral, quadrupole integral, or any other higher-order integral. However, for those higher moments, a common origin must be defined. This can be accomplished by calculating two centers of charge, one for all-positive and one for all-negative contributions to q_{KL}.[71] The common origin is then defined as the center of charge using the absolute values of these two charge distributions. Typically, all local moments to quadrupole are calculated for all atom and bond centers. With this choice of expansion centers, the multicenter multipole expansion (MME) converges rapidly in the sense that it also models higher-order molecular moments. The distributed moments add up to give the expectation value of the corresponding molecular moments from the wave function, and the distributed moments also include large portions of higher-order molecular moments.

This scheme for calculating the local moments is not unique, since the local charge distribution does not correspond to any observable of the system, but it does define a practical and compact description of the molecular charge distribution. The expansion scheme described above must be truncated at a suitable level in order for it to be used in molecular simulations of liquids. In some work, the atomic charges plus charges centered off the atoms have been used.[14,62] In other work, atomic charges and dipole moments have been adopted.[85,86] In this latter case, the local moments assigned to the bonds are moved to the nearest atoms and the moments of the atoms are changed accordingly. All local atomic quadrupoles are modeled by assigning a set of dipole moments to the nearby atoms. This modification of the atoms' local dipoles is made in such a way that the molecular dipole moment is unaffected.[86]

A completely different way to calculate the charge distribution is to fit point charges so as to reproduce the molecular electrostatic potential (MEP) around the molecule.[87−89] This method, which extracts charges from the MEP, is quite popular and has been frequently used in simulations along with an empirical Lennard−Jones term. However, if the aim of the modeling is high accuracy, a MME description of the electrostatic energy is more advantageous than fitting the MEP. One advantage of an MME description is that it does not suffer from penetration effect problems in determining the electrostatic energy. Penetration effects originate from the overlap of the wave functions of the interacting molecules and cannot be represented by any multipolar description. When determining accurate potentials, penetration effects from the electrostatic term are usually included in the exchange−repulsion term (vide infra). To avoid penetration effects, the MEP could be fitted on a grid at least 1 Å outside the van der Waals surface of the molecule. However, higher-order moments (octupoles, hexadecapoles, etc.) give only a small contribution at these distances and their effects at shorter distances may be poorly reproduced. Atomic charges (and higher-order moments) can be fitted from the MEP of a MME,[90−92] which eliminates the problem of penetration effects. A second problem with the MEP is that only atomic charges are usually fitted to it; higher-order moments are not included. However, a recent study concluded that at least atomic dipole moments must be included if the MEP is to be accurately described.[93] However, the MEP can be accurately described with charges alone if some are at sites off the atomic centers.[94] Benzene

provides a well-known example of the problems that can arise when only point charges are used.[95] In this case atomic charges located only on the atoms fail to reproduce the MEP. In addition to the advantages just listed, a MME expansion of the charge distribution is also more computationally efficient to obtain than fitting atomic charges to the MEP of the charge distribution.

An alternative approach for obtaining atomic properties involves considering the gradient of a higher-order molecular property for a set of points using classical electrostatics.[68] For example, for a set of N atomic point charges, q_i, the molecular dipole moment, μ_α, is given as

$$\mu_\alpha = \sum_{i=1}^{N} q_i r_i,\alpha \tag{14}$$

and the atomic charge may be obtained as

$$q_i = \frac{\partial \mu_\alpha}{\partial r_{i,\alpha}} \tag{15}$$

for $\alpha = x, y,$ or z. The gradient of the molecular dipole moment (the atomic polar tensor, APT) may be calculated by quantum chemical methods.[96] However, the diagonal terms of the quantum-chemically derived APT are not identical, although a definition like[68]

$$q_i = \frac{1}{3}\left(\frac{\partial \mu_x}{\partial r_{i,x}} + \frac{\partial \mu_y}{\partial r_{i,y}} + \frac{\partial \mu_z}{\partial r_{i,z}}\right) \tag{16}$$

will fulfill all the requirements for an atomic property. This definition of an atomic charge has been applied to some systems[97−100] where it has been noted that the APT charges behave much better with respect to the basis set than do Mulliken-like charges.[101] By appropriately modifying eq 14, this approach may be used for any atomic property.[68]

Applying this approach to a set of atomic charges and atomic dipole moments gives the molecular dipole moment as

$$\mu_\alpha = \sum_{i=1}^{N} (q_i r_{i,\alpha} + \mu_{i,\alpha}) \tag{17}$$

If it is furthermore assumed that the atomic properties depend on the molecular geometry, a component of the APT is given as

$$\frac{\partial \mu_\alpha}{\partial r_{j,\beta}} = \delta_{\alpha\beta} q_j + \frac{\partial q_i}{\partial r_{j,\beta}} r_{i,\alpha} + \frac{\partial \mu_{i,\alpha}}{\partial r_{j,\beta}} \tag{18}$$

The symmetry of some molecules can be utilized. For example, with a planar molecule, the out-of-plane components of the derivatives of the atomic properties in eq 18 are zero, and an atomic charge may be defined as[102]

$$q_i = \frac{\partial \mu_z}{\partial r_{i,z}} \tag{19}$$

where z is the out-of-plane component. This approach has also been applied to atomic dipole moments and geometry derivatives of atomic electrostatic moments.[102−105]

2.2.2. The Induction Energy

Inserting the form of $\hat{V}$ given in eq 7 into the polarization term in eq 5 gives the interaction between the charges on molecule 1 (2) and the induced moments of molecule 2 (1), assuming that overlap effects may be neglected. The leading term in the induction energy is due to the molecular polarizability and thus the corresponding molecular induced dipole moment arising from the electric fields of the other molecule. However, for a partitioning of molecular properties such as in eq 13, the distributed contributions to the molecular polarizability also contain in addition to the atomic polarizabilities, for example, atomic monopole−monopole polarizabilities (atomic capacitances), which as a response to a potential difference over the molecule results in induced atomic charges.[8]

Just as the definition of distributed multipole moments is not unique, so too is the definition of distributed polarizabilities not unique. Different methods of different complexity have been proposed to obtain the distributed polarizabilities.[80,106−115] However, very few have been used in constructing intermolecular potentials. The induced moment in the external field is the derivative of the second-order energy with respect to the field components, so in theory it should be straightforward to calculate polarizabilities. However, this has turned out not to be the case, and it is difficult to calculate distributed polarizabilities.[8] To do so it is apparently necessary to first define the matrix elements of the distributed multipole operator in terms of an integral over physical space. Different schemes to accomplish this have been suggested.[107−110]

A simple method for calculating local dipole polarizabilities according to Karlström will be briefly described.[106] This method has been frequently used in the construction of intermolecular potentials along the lines covered in this review. According to this method, the dipole polarizability is defined in an uncoupled Hartree−Fock approach as

$$\alpha_{\alpha\beta} = 4 \sum_i \sum_a \frac{\langle \psi_i | r_\alpha | \psi_a \rangle \langle \psi_i | r_\beta | \psi_a \rangle}{\epsilon_a - \epsilon_i} \tag{20}$$

where i denotes an occupied molecular orbital, a denotes an unoccupied molecular orbital, and ϵ_a and ϵ_i denote the corresponding orbital energies. Inserting eq 9 into eq 20 gives

$$\alpha_{\alpha\beta} = 4 \sum_{i,a} \frac{1}{\epsilon_a - \epsilon_i} \sum_{K,\mu_K} \sum_{L,\nu_L} \sum_{M,\zeta_M} \sum_{N,\lambda_N} c_{i\mu K} c_{a\nu L} c_{i\zeta M} c_{a\lambda N} \times \langle \chi_{\mu K} | r_\alpha | \chi_{\nu L} \rangle \langle \chi_{\zeta M} | r_\beta | \chi_{\lambda N} \rangle \tag{21}$$

The polarizabilities can be divided into four-center contributions as

$$\alpha_{\alpha\beta}^{KLMN} = 4\sum_{i,a}\frac{1}{\epsilon_a - \epsilon_i}\sum_{\mu_K}\sum_{\nu_L}\sum_{\zeta_M}\sum_{\lambda_N} c_{i\mu K}c_{a\nu L}c_{i\zeta M}c_{a\lambda N} \times \langle\chi_{\mu K}|r_\alpha|\chi_{\nu L}\rangle\langle\chi_{\zeta M}|r_\beta|\chi_{\lambda N}\rangle \quad (22)$$

while summation over the virtual orbitals gives

$$\alpha_{\alpha\beta}^{KM} = \sum_L\sum_N \alpha_{\alpha\beta}^{KLMN} \quad (23)$$

An origin must be defined in order to evaluate the local contributions of the transition dipoles integrals. In this analysis, the origin is defined as the molecular orbitals' center of charge[106]

$$X_{ij} = \frac{X_i + X_j}{2} \quad (24)$$

where X_i is the center of charge for orbital i. The molecular polarizability does not vary when different origins are chosen for the evaluation of the local contributions, but the local polarizabilities are very dependent on the choice. It has also been noted that it is important to use localized orbitals in this approach.[116]

A completely different way to calculate polarizabilities is to apply an electric field to a molecule and then calculate the difference in the electrostatic potential around the molecule induced by the applied field. The polarizabilities are fitted to reproduce the difference in electrostatic potential. This method is similar to fitting atomic charges to the MEP, and polarizabilities have recently been developed for some amino acids using this approach.[117,118]

The induction energy between two molecules (A and B) is calculated in classical electrostatics as[119]

$$E_{\text{class}}^{\text{ind}} = -\frac{1}{2}(\mathbf{F}_A^0\mu_B + \mathbf{F}_A^0\mu_A) \quad (25)$$

where $\mathbf{F}_A^0$ is the electric field from the permanent electrostatic moments of molecule A calculated at molecule B and μ_B is the induced dipole moment on molecule B due to the field generated by the permanent electrostatic moments of molecule A and the induced dipole moment on molecule A. $E_{\text{class}}^{\text{ind}}$ is usually calculated in an iterative manner. The induced moment on molecule A is calculated from the field generated by the permanent electrostatic moments of molecule B, and the induced moment on molecule B is calculated from the field generated by the permanent electrostatic moments of molecule A. Then, additional induced moments are calculated from the field generated by the induced moments from the prior iteration. This iterative procedure is continued until the total induced dipole moment in the molecules has converged. Note that $E_{\text{class}}^{\text{ind}}$ is different from the induction energy calculated from second-order intermolecular perturbation theory, since $E_{\text{class}}^{\text{ind}}$ also includes higher-order terms from the perturbation expansion.[120]

The derivation of the empirical potential parameters can be based on the assumption that the parameters are transferable from one molecular system to another, and these parameters often are regarded as atom-type parameters. Investigations have shown that there is little, if any, transferability of distributed multipoles.[121,122] To understand the transferability of the atomic electric moments and polarizabilities in more detail, we will assume that a molecule consists of interacting atoms. In addition to having a nuclear charge, each atom is regarded as a point with a spherically symmetric polarizability, a capacitance, and any other nonvanishing property which is consistent with the given symmetry of the unperturbed atom. Models for parameterizing the molecular polarizability tensor have been developed based on interacting point polarizabilities[113,123−126] and an additional atomic capacitances.[127,128] In the limit at which no external electric field is applied, the atomic dipole moments and the anisotropy of the atomic polarizabilities are due to the internal electric fields and thus are determined by the surrounding atoms in the molecule. Similarly, if atomic capacitances are included, the potential difference between the atoms will cause a charge flow from one atom to another and thus the atomic charges also can be determined from the interactions of each atom with the surrounding atoms. Thus, it should not be expected that atomic charges, dipole moments, and polarizability tensors can be treated as atom-type parameters since they can be regarded as originating from interactions with neighboring atoms in the molecule. Perhaps, instead, the concept of interacting atoms can be used to determine atom-type parameters that in turn can be adopted to obtain the atomic charges, dipole moments, and polarizability tensors of the molecule of interest.

2.2.3. The Dispersion Energy

The dispersion energy of a system can be described in a number of different ways.[61,131−134] One method that has been shown to work very well for small molecules is to use C_n ($n = 6-10$) coefficients from quantum chemical calculations[64,131]

$$E^{\text{disp}} = -\sum_{n=6}^{10}\sum_{l_1l_2k_1k_2}\frac{C_n(l_1l_2k_1k_2)}{R^n}\bar{S}_{l_1l_2j}^{k_1k_2}(\omega_A\omega_B\omega)\, f_n(a,R) \quad (26)$$

where $\bar{S}_{l_1l_2j}^{k_1k_2}(\omega_A\omega_B\omega)$ are the normalized real components of Stone's orientational S functions,[8] R is the distance been centers of mass, and $f_n(a,R)$ is a damping function.[129] In recent work, Hodges et al.[135] described the dispersion energy as

$$E^{\text{disp}} = -G(R)\times\frac{C_6}{R^6} \quad (27)$$

where $G(R)$ describes both the effects of the terms in higher powers of R^{-1} at intermediate range and the damping. This $G(R)$ term is fitted to SAPT calculations of the dispersion energy.

Alternatively, a simple expression of the dispersion energy can be derived from perturbation theory. The leading term in the dispersion intermolecular interactions in eq 5 is the dipole−dipole term[67]

$$E^{\mathrm{disp}} = -\sum_{\alpha\beta\gamma\delta}^{3} T_{\alpha\beta}T_{\gamma\delta} \times \sum_{a>0}\sum_{b>0} \frac{\langle\psi_0^1\psi_0^2|\mu_{1\alpha}\mu_{2\beta}|\psi_{(a)}^1\psi_{(b)}^2\rangle\langle\psi_{(a)}^1\psi_{(b)}^2|\mu_{1\gamma}\mu_{2\delta}|\psi_0^1\psi_0^2\rangle}{\epsilon_{(a)}^1 + \epsilon_{(b)}^2 - \epsilon_0^1 - \epsilon_0^1\epsilon} \quad (28)$$

To separate the sum over molecules 1 and 2 [$\sum_1\sum_2$] into a product [$(\sum_1)(\sum_2)$] of isolated molecular terms, the denominator has to be approximated. For every excited state a, the excitation energy ($\epsilon_a^1 - \epsilon_0^1$) is approximated by $\bar{E}_1$, where $\bar{E}_1$ is the average excitation energy for molecule 1. This type of denominator approximation was first used by Unsöld.[136] Using this approximation, E^{disp} can be rewritten as

$$E^{\mathrm{disp}} = -4\frac{\bar{E}_1\bar{E}_2}{\bar{E}_1 + \bar{E}_2}\sum_{\alpha\beta\gamma\delta}^{3} T_{\alpha\beta}T_{\gamma\delta} \times \sum_{a>0}\frac{\langle\psi_0^1|\mu_{1\alpha}|\psi_a^1\rangle\langle\psi_a^1|\mu_{1\gamma}|\psi_0^1\rangle}{\bar{E}_1} \sum_{b>0}\frac{\langle\psi_0^2|\mu_{2\beta}|\psi_b^2\rangle\langle\psi_b^2|\mu_{2\gamma\delta}|\psi_0^2\rangle}{\bar{E}_2} \quad (29)$$

Replacing E_1 and $\bar{E}_2$ with the excitation energies and identifying the last terms as molecular polarizabilities gives

$$E^{\mathrm{disp}} = \frac{1}{4}\frac{\bar{E}_1\bar{E}_2}{\bar{E}_1 + \bar{E}_2}\sum_{\alpha\beta\gamma\delta}^{3} T_{\alpha\beta}T_{\gamma\delta}\alpha_{\alpha\gamma}\alpha_{\beta\delta} \quad (30)$$

which is a dispersion formula of the London type,[67] where T is the dipole−dipole propagator. However, in a distributed model of the polarizability, contributions also arise from the monopole polarizabilities.[8] The average excitation energies can be replaced by the average HF ionization energies. Equation 30 is derived with the assumption that the electron clouds of the molecules do not overlap. However, overlap and exchange effects do weaken the dispersion term at short and medium ranges. The damping function derived by Tang et al. is used to correct for these effects.[129] Dispersion terms based on this approach have been used in several studies.[14,61,62,85,137]

2.2.4. The Exchange–Repulsion Energy

The RS perturbation theory, which is truncated after the second-order term, does not take into account exchange effects between molecules. Therefore, it has to be replaced by exchange−perturbation theory that takes into account the exchange between the electron clouds at shorter distances. Several different perturbation theories have been developed.[7,8] In their book, Margenau and Kestner[4] show that the Heitler−London method applied to the hydrogen dimer in the triplet state has an exchange−repulsion term that behaves as $S^2/(1 - S^2)$, where S is the electronic overlap. The term $S^2/(1 - S^2)$ can be expanded in a power series to $\alpha S^2 + \beta S^4 + \gamma S^6$, ..., where α, β, and γ are constants. In the original NEMO scheme,[13] this model was used to describe the exchange−repulsion term. However, it has been abandoned in later versions since it is computationally expensive. Since the exchange−repulsion energy may be approximated as being proportional to the square of the overlap and the wave function of the interacting monomers decays exponentially, it is logical to describe the exchange−repulsion as an exponentially decaying function of the atom−atom distance. It should be noted that if an exponential function is used to describe the exchange−repulsion energy, the total interaction energy between two atoms can become infinitely negative due to the attractive energy terms when the atoms come very close to each other. In practice this is normally not a problem since the exponential exchange−repulsion term prohibits the atoms from coming too close to each other. However, an extra short-range repulsion term, such as a term proportional to R^{-21},[86] could be added to counteract any close approach of atoms. An exchange−repulsion term that takes into account the anisotropy of the atoms would, of course, be more accurate than an isotropic atom−atom exchange−repulsion term. However, such an anisotropic exchange−repulsion also would be computationally demanding. Two different approaches have been used to fit the exchange−repulsion parameters. One possibility is to fit the parameters to HF quantum chemical energies minus the classic electrostatic and inductive contributions from local multicenter multipole moments and polarizabilities.[13] The quantum chemical energies have to be corrected for the basis-set superposition error (BSSE).[138] Thus, in this model the exchange−repulsion term also includes charge-transfer contributions and overlap effects. It recently was shown that the parameters could be fitted more efficiently if the atomic size was included in the fit.[86,139] Brdarski and Karlström[86] showed that the quality of the fit of the exchange−repulsion energy can be improved significantly when the sizes of the atoms are estimated from the ratio of their atomic second moment and their atomic valence charge. This ratio has the dimension of length squared and can be used as a measure of the extension of the electron cloud in the vicinity of the considered atom. By adding this quantity for two atoms and taking the inverse of the square root of the sum, a length scale can be defined. Using this length scale and assuming that the exchange−repulsion between two atoms is proportional to the product of their valence charges, it is possible to define atom-type parameters which describe the exchange−repulsion energy accurately.[86]

Another method for determining the exchange−repulsion energy is to fit the exchange−repulsion parameters to the first-order energy in IMPT[53] minus the classical electrostatic energy from the local multicenter multipole moments[63−65,140,141]

$$U_{\mathrm{ex-rep}}^{AB} = \sum_{a\in A}\sum_{a\in B} K\exp[-\alpha_{ab}(R_{ab} - \rho_{ab}(\omega_{ab}))] \quad (31)$$

where $K = 10^{-3}$ Hartree and the function $\rho_{ab}(\omega_{ab})$ is expanded in terms of the orientational $\bar{S}$ functions[8]

$$\rho_{ab}(\omega_{ab}) = \sum_{l_a,l_b,j,k_a,k_b} \rho_{l_a,l_b,j}^{k_a,k_b} \bar{S}_{l_a,l_b,j}^{k_a,k_b} \qquad (32)$$

Stone et al. successfully used a probe atom to speed up calculation of the exchange−repulsion parameters.[140,141] In this method, the exchange−repulsion parameters were calculated between the molecules and the probe atom. From these parameters, the exchange−repulsion parameters between the molecules then were extracted via combination rules. More recently, Stone et al. started to fit the exchange−repulsion parameters to the first-order energy in SAPT.[141] If the exchange−repulsion parameters are fitted to the first-order energy in IMPT, only the overlap effects originating from the electrostatics will be included whereas the overlap correction to the induction interaction is ignored. The charge-transfer contribution in IMPT is fitted separately.[69] A more empirical model that describes the exchange−repulsion energy has been developed by Wheatley and Price.[142,143] In their model the exchange−repulsion term is an exponential function of the electron density overlap between the two molecules.

3. Molecular Clusters

Interest in molecular clusters has increased over the last several years. New experimental techniques and faster computers have made it possible to study clusters much more accurately than was previously possible. The accurate intermolecular potentials constructed from perturbation theory have made a significant contribution to the understanding of the properties of molecular clusters. Accurate intermolecular potentials with explicit polarizabilities have been especially useful for studying clusters with three or more molecules, since many-body contributions are included in the induction term. Accurate potentials for dimers also can be fitted to quantum chemical calculations without having explicit polarizabilities in the potential[144] or they can be fitted directly from experimental spectroscopic data.[145,146] Fitting a potential to experimental data is problematic in that the interacting molecules have rigid monomer geometries; thus, any effects on the spectra from the deformation of the monomers must be included. So far most intermolecular potentials have been determined by taking into account only the inductive many-body effects. However, if spectroscopic accuracy is the goal, the intermolecular potentials used to describe clusters must also describe other many-body effects.[147] Many-body effects contribute to the dispersion,[54,148,149] exchange−repulsion,[150,151] and mixing[152,153] terms. Some of the cluster studies performed will be briefly described here. Other clusters that have been successfully modeled using accurate intermolecular potentials constructed from perturbation theory are the HCl dimer,[154,139] the CO dimer,[155] formamide clusters,[156] cyanoacetylene clusters,[157] acetonitrile clusters,[158] and hydronium−water clusters.[159] Intermolecular potentials have also been used to predict the far-infrared spectra of various bimolecular complexes[160,161] along with their second dielectric virial coefficients.[162] Stone et al. developed the software program ORIENT,[163] by which properties of clusters can be studied. ORIENT can handle a variety of different types of intermolecular potentials, and derivatives up to the second order are analytically calculated.[164]

3.1. Water Clusters

In the past few years there has been a great deal of interest, both from experimentalists and theoreticians, in small water clusters. At least 60 theoretical and 15 experimental studies on this topic have been recently published.[165] New experimental data has been obtained by far-IR vibration−rotation spectroscopy.[166] Recently, it has been noted that no existing water potential which has been designed for liquid simulations can reproduce the rotational−vibrational spectra of the water dimer.[167] In our opinion this is not surprising since an intermolecular potential has to have a simple functional form if it is to be useful in a simulation, and a simple functional form obviously sets a limit of how accurate a potential can be. Two families of water potentials have been developed from perturbation theory water. These are the NEMO water potentials, which have mainly been developed for bulk water simulations,[14,61,85,168] and the ASP potentials which mainly have been developed for studies of small water clusters.[63,64,169] The complexities of these two types of potentials are quite different. For example, the ASP potentials have a much more complex functional form than the NEMO potentials. It has been shown that the ASP−W4 potential is the best existing water potential for describing the dimer,[64] with the possible exception of a new water potential which is fitted to reproduce rotational−vibrational spectroscopic data.[145] The ASP−W4 potential describes the stationary points on the water dimer potential-energy surface well and gives a second virial coefficient that is in excellent agreement with experimental data. The ASP−W4 water potential has electrostatic moments up to the hexadecapole level that are centered on the atoms, polarizabilities up to the quadrupole−quadrupole level that are sited on the oxygen, and anisotropic repulsion and dispersion parameters.

It is important to compare energies from constructed intermolecular potentials with ab initio calculations of high accuracy for systems larger than the dimer, since this is the only way to test how well the constructed potential can reproduce many-body effects. High-quality ab initio data for molecular clusters have recently become available, making this type of comparison possible. The induction term is the most important many-body term when dealing with hydrogen-bonded clusters.

Both experiments and calculations yield a cyclic homodromic structure for the trimer and the tetramer at the energy minimum. (A homodromic structure occurs when all the water molecules are both hydrogen donors and acceptors.) The global minimum for the water trimer is given in Figure 1, while the global minimum for the tetramer is given in Figure 2.

The nonbonded hydrogens that are above the plane, below the plane, and in the plane are termed

Table 1. Total Energy and Many-Body Terms for the Energy Minima of the Trimer and Tetramer[a]

	$E^{tot}(H_2O)_3$	$E^{3-body}(H_2O)_3$	$E^{tot}(H_2O)_4$	$E^{3-body}(H_2O)_4$	$E^{4-body}(H_2O)_4$
tNEMO[b]	−14.52	−1.81	−26.50	−5.80	−0.61
ASP-W4[c]	−14.74	−2.14	−25.50	−5.78	−0.79
MP2[c]	−14.25	−2.45	−25.33	−6.23	−0.54
CCSD(T)[d]	−14.00	−2.37	−24.75	−6.08	−0.56

[a] All energies are given in kcal/mol. [b] Reference 168. [c] Reference 169. [d] Reference 165.

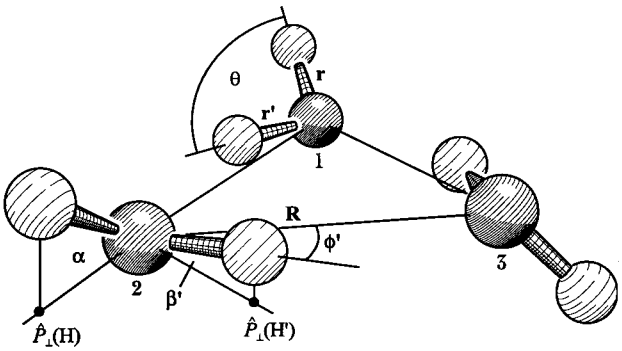

Figure 1. Global minimum energy structure of the cyclic homodromic water trimer (*uud*). (Reprinted with permission from *Mol. Phys.* **1997**, *90* (2), 277−287. Taylor & Francis. http://www.tandf.co.uk/journals.)

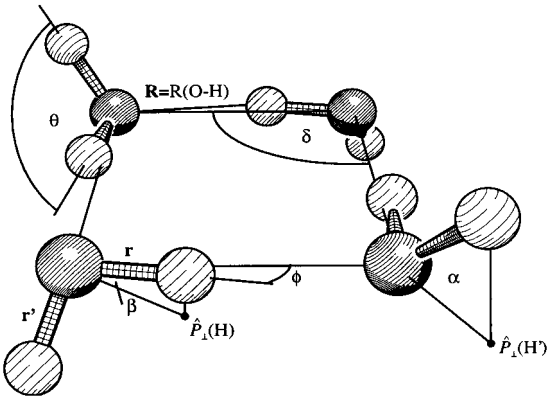

Figure 2. Global minimum energy structure of the cyclic homodromic water tetramer (*udud*). (Reprinted with permission from *Mol. Phys.* **1997**, *90* (2), 277−287. Tyalor & Francis. http://www.tandf.co.uk/journals.)

u (up), *d* (down), and *p* (planar), respectively. Thus, the minimum structures for the trimer and tetramer are denoted (*uud*) and (*udud*), respectively.

To our knowledge, of all the existing polarizable water potentials, only the ASP and NEMO potentials have many-body contributions that have been compared to accurate quantum chemical data. However, in a comparison by Alkorta et al.,[170] the NEMO potential was the polarizable water potential that most accurately described the induction energy of the water dimer. It should be noted that the induction term is the only many-body term in the potentials; many-body contributions to the dispersion and exchange−repulsion energy are omitted. The induction term is the most important many-body term for water clusters. Three-body corrections to the exchange−repulsion energy are of some importance for the water trimer, while three-body corrections to the dispersion energy are of negligible importance.[171,165] A comparison of the ASP and NEMO potentials is given in Table 1. Both potentials perform well, which is a verification that potentials constructed with explicit polarizabilities, where the polarizabilities are derived directly from the wave function, accurately describe many-body effects in water clusters.

The low-energy region of the potential-energy surface (PES) has been investigated for the water trimer[165,172−176] and tetramer.[177,165] Several distinct low-lying stationary points have been located on these surfaces. These stationary points represent cyclic and homodromic structures and differ mainly in the positions of the "free" O−H bonds relative to the O_3 (O_4) plane.

To determine how well the NEMO intermolecular water potential performed, it was used to calculate energies, structures, and harmonic vibrational frequencies and these were compared to the corresponding ab initio data.[168] The tNEMO potential was constructed along the lines described in the theory section. The charge distribution was described with multipole moments up to rank 2 on the atoms. Dipole−dipole polarizability tensors were sited on the atoms, and the dispersion was described using a London term. The exchange−repulsion was defined as being proportional to the overlap of the wave functions of the monomers. The other two NEMO potentials (fvcNEMO[14] and fdiNEMO[85]) are simplified versions of tNEMO and are suitable for simulations. A comparison of the NEMO results with some of the most popular water potentials (SPC,[178] TIP4P,[179] MCY,[20] and EPEN[180]) revealed that only the NEMO potential was able to reproduce the correct ordering of the stationary points for the water trimer.[168,181] However, it should be pointed out that the other potentials have a much simpler functional form than the NEMO potential and that the TIP4P and SPC potentials were specifically constructed to reproduce liquid water data. Also, it was recently shown that DFT calculations are not able to reproduce the right order for the stationary points.[165]

Table 2 compares the different NEMO potentials with ab initio calculations for the water trimer. As can be seen, the NEMO potentials reproduce the ab initio results well. Only one high-quality ab initio calculation has been performed for the stationary points of the cyclic homodromic tetramer which includes all the interesting stationary points in the PES.[177] The quantum chemical and the NEMO results are compared in Table 3. From this it can be seen that the many-body effects are crucial to describing the PES for the cyclic homodromic tetramer.[168]

Both the ASP and NEMO potentials have problems describing large water clusters. The fvc version of NEMO has been compared to local MP2 (LMP2) calculations by Hartke et al.[182] It was found that fvcNEMO correctly predicts the minimum for the

Table 2. Energetics for the Cyclic Homodromic Water Trimer[a]

	{*uud*}	{*upd*}	{*uuu*}	{*ppp*}
tNEMO[b]	−14.53	0.17	0.75	1.02
fvcNEMO[c]	−13.47	0.16	0.74	0.97
fdiNEMO[b]	−14.89	0.10	0.53	0.61
MP2-R12[c]	−16.32	0.22	0.79	1.22
MP2[d]	−14.76			1.05
CCSD[e]	−16.70	0.30	0.85	1.67
MP2[f]	−13.91	0.04	0.50	0.51
CCSD(T)[g]	−14.00	0.25	0.77	1.41

[a] All Energies Are Given in kcal/mol. The absolute values of the dissociation energies are given for the {*uud*} conformer (global minimum), while for the other stationary points the energy differences relative to {*uud*} are given. [b] Reference 168. [c] Reference 174. [d] Reference 175. [e] Reference 176. [f] Reference 172. [g] Reference 165.

water pentamer. However, fvcNEMO predicts the wrong minimum for the hexamer. fvcNEMO predicts the cyclic hexamer to be the most stable structure, while the LMP2 calculations predict a prism structure to be the most stable. fvcNEMO overestimates the stability of the cyclic hexamer by approximately 5% compared to the LMP2 calculations. However, it should be mentioned that LMP2 is a new method and its general reliability is not yet firmly established. It has also been found that the ASP water potentials predict a cage structure as the minimum for the water pentamer instead of the experimentally observed cyclic structure.[183] However, these considerations are valid for potential-energy surfaces and are not directly applicable to the experimentally observed structures since no account is given to the zero-point vibrational energies.

3.2. Benzene Clusters

The benzene−benzene interaction is of key importance as a prototype for the interactions prevailing in aromatic systems. A new benzene−benzene intermolecular potential has been created using the NEMO methodology.[184] This potential was calibrated to reproduce the benzene dimer interaction energy at the CCSD(T) level.[185] The potential-energy surfaces were investigated for the dimer, trimer, and tetramer. The energy of the dimer was found to be −1.7 kcal/mol, and the minima structure was found to be T-shaped. The parallel displaced structure, which previously has been suggested to be the global minimum on the PES, was found to be a first-order transition state with an energy of −1.2 kcal/mol. It should be pointed out that a T-shaped minimum structure was suggested in 1983 based on an approach similar to NEMO.[186] The benzene trimer was also investigated using the new potential.[187] The global minimum for the trimer was shown to be a cyclic structure consisting of three deformed T-shaped bonds. The interaction energy for this species is −5.1 kcal/mol. The cyclic structure is in agreement with both experiment[188] and earlier theoretical studies.[189] Finally, the benzene tetramer was investigated. The most stable structure for the tetramer was shown to be a 4-fold cyclic structure with an energy of −8.1 kcal/mol. However, there also are three tetramer structures which each have an energy between −7.3 and −7.9 kcal/mol These structures each consist of three benzenes arranged in a triangle with the fourth benzene binding to that triangle. Experimentally, the latter type of structures have been detected.[188] This discrepancy between experimental and theoretical results could be due to entropic and kinetic effects as well as to the potential not being accurate enough. For example, many-body contributions to the dispersion and exchange−repulsion term are not included in the potential, and these contributions could be of importance for benzene clusters, since the dispersion energy is the predominant attractive energy term.

3.3. HF Clusters

Hydrogen fluoride clusters have been the subject of numerous experimental and theoretical calculations. Like water, hydrogen fluoride is a strongly hydrogen-bonded system. A new intermolecular potential designed for studies of hydrogen fluoride clusters has recently been constructed from ab initio calculations by Hodges et al.[65] For the dimer, the interaction energy is −4.5 kcal/mol, which is similar to both high-level ab initio calculations[190] and experiment.[191] The dimer has a planar hydrogen-bonded structure with C_s symmetry, and the transition state between the two symmetry equivalent minima has an energy of −1.0 kcal/mol. It also was found that all the species from the trimer through the hexamer have cyclic structures. This could be attributed to favorable many-body interactions and maximization of the number of hydrogen bonds. No rearrangements were found in the trimer, tetramer, or pentamer that would give rise to significant tunneling splittings.

3.4. HCN Clusters

Hydrogen cyanide clusters have been frequently studied both experimentally and theoretically. An accurate intermolecular potential has recently been constructed by Cabaleiro-Lago et al.[192] for the HCN dimer and used in studies of HCN clusters of various

Table 3. Energetics for the Cyclic Homodromic Water Tetramer[a]

	{*udud*}	{*uudd*}	{*uupd*}	{*uudp*}	{*updp*}	{*uppd*}	{*uuuu*}	{*pppp*}
tNEMO[b]	−26.50	1.08	1.50	1.51	1.68	1.88	2.80	3.39
fvcNEMO[b]	−24.56	0.78	0.95	0.95	1.06	1.00	1.73	1.84
fdiNEMO[b]	−26.30	0.71	0.84	0.85	0.99	0.87	1.46	1.50
MP2-R12[c]	−28.10	0.93	1.24	1.24	1.40	1.38	2.17	2.79
CCSD(T)[d]	−24.75							3.06

[a] All energies are given in kcal/mol. The absolute values of the dissociation energies are given for the {*udud*} conformer (global minimum), while for the other stationary points the energy differences relative to {*udud*} are given. [b] Reference 168. [c] Reference 177. [d] Reference 165.

sizes. The HCN dimer has a linear structure with an interaction energy of −4.4 kcal/mol. A linear structure also was found to be the global minimum for the trimer, while a cyclic structure was found to be a local minimum with a slightly higher energy. These results are in agreement with quantum chemical calculations. For larger clusters, a number of minima having different structures were found. However, for 4−8 HCN molecules, the global minima always corresponded to a cyclic structure.

King et al. suggested that the hydrogen bonding in HCN clusters is largely charge-transfer in origin.[193] However, Stone et al. convincingly showed that charge-transfer effects are small and that electrostatic and induction interactions are actually the main contributors to the hydrogen bonding.[194]

4. Molecule–Surface Interactions

Adsorption on surfaces is an important topic since it has applications in areas ranging from atmospheric chemistry to industrial catalytic reactions. Surface adsorption can be divided into two types: chemadsorption, which could be studied with methods such as density functional methods, and physadsorption, which can be studied using ordinary intermolecular potentials. Thus far, physadsorption on crystals mainly has been studied using nonpolarizable intermolecular potentials. One problem with many of these empirical studies is that the ion charges on the surface have been in strong disagreement with those obtained from quantum chemical calculations.[195] Being able to accurately model polarization effects is crucial to studying surface interactions in an inhomogeneous environment. This is in contrast to systems such as a neat liquid where the permanent electrostatic moments are often scaled to get the correct liquid properties which allows a pairwise representation of the interactions to be retained.

4.1. Intermolecular Potentials

The first potentials constructed using IMPT recently have been developed for the adsorption of small molecules on crystal surfaces. H_2O adsorption on NaCl[196] and MgO surfaces[195] has been studied, as has CO adsorption on NaCl[197,198] and SO_2 adsorption on NaCl.[199] The methodology for constructing the water−surface potentials will be briefly discussed, since it differs in part from the derivation of potentials between two isolated molecules. The exchange−repulsion parameters for the cation−water interaction were calculated as the difference between the first-order interaction energy in IMPT and the classical electrostatic energy between the cation and the multicenter multipole expansion for water. For the anion, a more elaborate model was used in the IMPT calculations. The calculations were performed with the anion surrounded by five cations, one in each direction except the positive z direction. More distant ions were modeled by point charges. The dispersion term was calculated using C_6 coefficients obtained at the coupled Hartree−Fock level. When the model developed by Fowler and Madden was used,[200] the calculation for the cation was straightforward while the anion calculation was again more complicated. The anion was embedded in a cluster of cations described by a minimal basis set, and the whole cluster was surrounded by point charges.

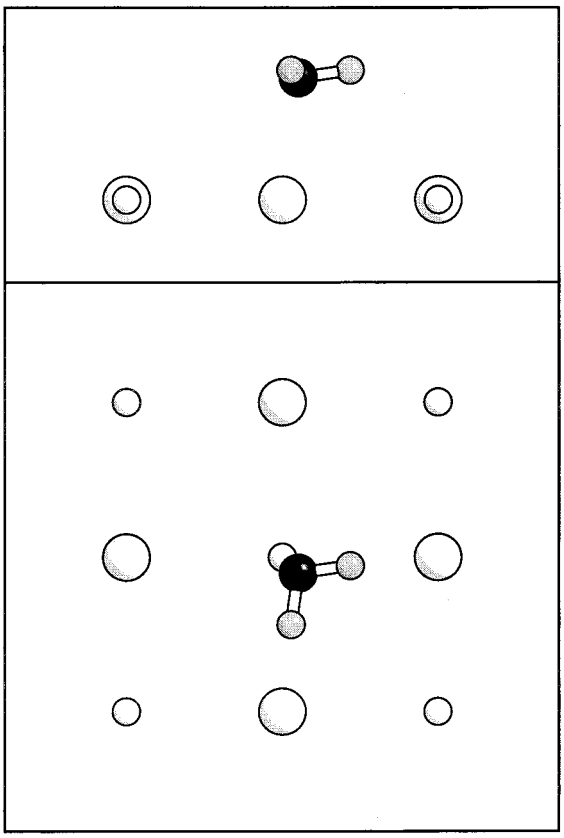

Figure 3. Minimum energy structure for a water molecule on the NaCl(001) surface. (Energy −9.5 kcal/mol.) (Reprinted with permission from ref 196. Copyright 1999 American Institute of Physics.)

4.2. Applications

The H_2O−NaCl potential resulted in an interaction energy of −9.5 kcal/mol at the potential minimum,[196] and this energy is close to the rather uncertain experimental value of -10.3 ± 2.5 kcal/mol.[201] At the potential minimum, the water molecule is adsorbed on the surface with the oxygen above a Na^+ ion and the hydrogens pointing toward Cl^- ions. This structure is shown in Figure 3.

A wealth of cluster, one-dimensional chain, and monolayer structures were investigated using the ASP−W4 potential which has been described above[169] for the water−water interaction. It was found that four water molecules could form a very stable tetramer on the surface with a binding energy of 13.2 kcal/mol per water molecule. Monolayer structures with coverages of 1.0 and 1.5 water molecules per unit cell were investigated. Different monolayer structures have been found when using different experimental techniques at cryogenic temperatures.[202−204] In the new theoretical study it was found that there exists a wealth of monolayer structures with approximately the same energy, all of which could coexist on the surface.[196] The presence of different structures with similar energies could lead to a system that is very sensitive to experimental

conditions, which could explain why different experimental techniques predict different structures. The monolayer structures each have an energy of approximately −12.5 kcal/mol per water molecule.

Water adsorbed on a MgO(001) surface was investigated using a similar methodology.[195] The binding energy for a single molecule on the MgO(001) surface was calculated to be 15.6 kcal/mol. In the minimum energy structure, the O atom of the water molecule is situated above a Mg^{2+} ion, with the molecular plane almost parallel to the surface and the OH bonds directed toward the O^{2-} ions. Several monolayer structures were investigated at a coverage of 1.0 water molecule per MgO unit. The *p*(2H1) structure had a slightly lower energy (−21.2 kcal/mol per water molecule) than that found experimentally for the *pg*(3H2) structure (−20.8 kcal/mol per water molecule).[205] Calculations indicated that this discrepancy could be due to a neglect of the intermolecular vibrational effects. However, the energy difference between these two monolayer structures is within the error bars of the potentials. The calculated enthalpy of desorption and the distance between the monolayer and the substrate were both in agreement with experimental results. Water binds much more tightly to the MgO(001) surface than to the NaCl(001) surface for two reasons. First, the electrostatic interaction between water and the MgO substrate is larger than that between water and the NaCl substrate due to the larger MgO charges. Second, the MgO ion−ion distance is 2.98 Å, which favors efficient hydrogen bonding between the adsorbed water molecules. (The O−O distance in the water−water interactions is approximately 3 Å.) The ion−ion distance in NaCl is 3.98 Å, which is not favorable for efficient hydrogen bonding between the water molecules on the surface.

Meredith and Stone studied the adsorption of CO on NaCl.[198] Two minima were found for a single CO molecule adsorbed on the NaCl surface. In both cases, the molecule is adsorbed over a Na^+ ion with its molecular axis perpendicular to the surface. However, in one case the C end of the molecule points down (−3.8 kcal/mol), while in the other case the O end of the molecule is down (−1.8 kcal/mol). It was also found that induction contributes significantly to the overall binding energy. CO's preference for an upright structure arises from electrostatic interactions. An investigation of CO monolayers with *p*(1*X*1) and *p*(2*X*1) structures showed that two competing effects influence the structure of the adlayer on the NaCl(001) surface. The lateral interactions within the monolayer favor a tilted structure, while the molecule−substrate interactions favor an upright geometry. The calculated enthalpy of desorption for these structures was in agreement with experiment.[206] The energy difference between the *p*(1*X*1) and *p*(2*X*1) structures is very small. This is compatible with experimental findings at 35 K that showed a phase transition, from a *p*(2*X*1) structure to a *p*(1*X*1) structure.[207]

In a combined experimental and theoretical study Berg et al.[199] investigated the adsorption of SO_2 on NaCl at cryogenic temperatures. Accurate potentials were used in MC simulations at coverages of 0.5 and 1.0 SO_2 molecule per NaCl unit. At both coverages a two-dimensional condensate developed, which is consistent with polarized infrared spectroscopy experiments.

5. Simulations of Liquids and Solutions

Perhaps the most important application of intermolecular potentials is to model the interaction energies and forces between molecules in liquids and solutions. The behavior of a solution is due to a subtle balance between entropy and enthalpy effects, and it is therefore obvious that the reliability of the interaction potential is crucial in describing these systems. However, in a molecular dynamics (MD) simulation, the interaction energy and the forces have to be calculated over and over again for hundreds or even thousands of particles. A typical time step in a classical MD simulation is on the order of 1 fs, and the simulation time required to achieve accurate statistical mechanical ensemble averages is on the order of 10 ps to many ns, depending on the system and the property of interest.[11] Therefore, a computationally efficient representation of the interaction potential is needed, and the choice of representation will be a compromise between accuracy and efficiency. In a perturbation approach to intermolecular interactions, the considerations that affects the accuracy of the interaction potential are as follows. (1) The choice of which terms to include from the perturbation expansion of the interaction energy. (2) The accuracy of the potential parameters. As is true in quantum chemical calculations of any molecular property, the basis-set dependence and the inclusion of electron correlation has to be considered in detail. The calculation of potential parameters was discussed in section 2.2. (3) The representation of the potential in the simulation. The functional form of the interaction energies and forces given by perturbation theory may be too complex to be adopted directly in a many-particle simulation, and a simplified form has to be adopted. The latter consideration will be discussed in some detail.

NEMO is an approach which includes the ideas of intermolecular interactions as described by perturbation theory in a molecular dynamics program.[13,208] In the original work, the electrostatics were represented by point charges distributed to sites in addition to the atomic sites in order to accurately reproduce the molecular dipole and quadrupole moments.[13,14,209,210] Furthermore, in the simulations, the atomic polarizability tensors were approximated using isotropic polarizabilities in line with early work on adopting polarizabilities in molecular simulations.[211] However, it has been demonstrated that a computationally more efficient approach is to represent the electrostatic and induction forces by using dipole moments and polarizability tensors on atoms along with the atomic charges rather than by using a larger number of atomic charges.[85] It is clear that more complex intermolecular potentials are required to accurately describe the forces in soft condensed matter, and perturbation theory provides a route to systematically increase the accuracy of the force fields.

Perhaps the most important advantage of using perturbation theory-derived intermolecular potentials in MD simulations is that this allows the polarizabilities to be included in a straightforward manner. In simulations of neat liquids, it may be justifiable to neglect many-body interactions by rescaling the permanent atomic charges in order to obtain the correct electrostatic moments for the molecules in the liquid. However, with solvated molecules and especially with solvated ions, as well as with interactions at surfaces (see section 4, the polarization of the neighboring molecules by the species of interest is substantial due to the inhomogeneity of the surroundings and the many-body interactions should not be neglected. However, the inclusion of explicit polarizabilities in a force field for MD simulations is in principle a computationally demanding task. The atomic induced dipole moment, $\mu_{\alpha,i}^{\mathrm{ind}}$, is given as

$$\mu_{\alpha,i}^{\mathrm{ind}} = \alpha_{\alpha\beta,i} \left(E_{\beta,i}^{\mathrm{stat}} + \sum_j T_{\gamma,ij}^2 \mu_{\gamma,j}^{\mathrm{ind}}\right) \qquad (33)$$

where $\alpha_{\alpha\beta,i}$ is the atomic polarizability, $E_{\beta,i}^{\mathrm{stat}}$ is the static electric field arising from the permanent atomic electric moments on all of the other molecules, and $\sum_j T_{\gamma,ij}^2 \mu_{\gamma,j}^{\mathrm{ind}}$ is the electric field arising from the atomic induced dipole moments on those same molecules. Thus, the atomic induced dipole moment is a true many-body effect. Within the Born−Oppenheimer approximation, the electronic response is instantaneous compared to the nuclear motion. The set of coupled equations for the atomic induced dipole moments therefore should be solved, preferably by an iterative procedure, in each time step of the MD simulation. In an MD simulation, however, we are normally interested in static properties or in properties that relax on a time scale different from the approximately 1 fs time step. Thus, it is not a problem if the electronic response relaxes on the same time scale as the time step. Therefore, the methods that are used for propagating the atomic positions also can be used for propagating the atomic induced dipole moments and the computer-demanding iterative procedure can be avoided.[117,212−216] The additional calculation of forces and torques arising from atomic polarizabilities is no more complicated than the calculation of permanent dipole moments, which can be shown using classical response theory.[85,217] General formulas for the electrostatic forces and torques have been previously presented,[164,218] and the pairwise anisotropic site potentials have been used in liquid simulations for some time.[219−223] In addition, long-range interactions based on the Ewald summation and reaction field methods recently have been included recently for potentials with atomic charges, dipole moments, and polarizability tensors.[224,225]

An atomic polarizability only modifies the atomic dipole moment; however, the atomic charges are also affected by intermolecular interactions. Charge flow within a molecule is due to the potential difference over the entire molecule and may be modeled using atomic capacitances (monopole polarizabilities). The approach presented by Stone for partitioning the molecular dipole polarizability includes both atomic monopole and dipole polarizabilities.[8,107] The atomic charges have been modified in response to the surrounding molecules in some simulations,[212,215,226,227] and both atomic capacitances and polarizabilities have been included explicitly in MD simulations of liquids.[228]

If a perturbation approach converges, it gives the exact quantum mechanical interaction energy. An alternative approach would be to solve the electronic part of the Schrödinger equation for the entire system of molecules in each time step. However, this is prohibitively computer-demanding. The Car−Parrinello (CP) method[39,229] provides a more viable approach. In this method the electronic structure is calculated for each time step in a local-density approximation of the density functional theory. For simulations of some systems, such as those where covalent bonds are broken or formed, the perturbation approach is clearly not valid. However, for systems where only intermolecular interactions are considered, the changes in the electronic structure can be modeled using polarizabilities, which allows the interaction energies and forces to be calculated using only a fraction of the computer resources needed by the CP method. Furthermore, if a system such as a reaction is studied, the part of the system that cannot be treated by intermolecular perturbation theory is often limited to only a few molecules. A suitable approach, which is in line with intermolecular perturbation theory, would be to calculate the potential parameters for the reactants in each time step and use those potentials to obtain the interactions of the molecules with the bulk part of the system. Initial studies along these lines have been carried out for a water molecule in liquid water.[230−232] Since a perturbation approach and the local-density approximation are based on completely different approximations, studies with the two methods should be regarded as complementary.

A discussion of the simulations of some systems follows. It should be emphasized that almost all simulations have been carried using empirical or semiempirical potentials without the explicit inclusion of many-body effects. In this work, however, the discussion will be restricted to simulations based on intermolecular potentials obtained from perturbation theory, that is, those in which all the potential parameters have been calculated using perturbational methods and for which the potential consists of (at least) electrostatic, induction, dispersion, and repulsion contributions. Simulations of this type have so far been quite rare, and those which have been performed are briefly discussed. The simulation of 1,2-dimethoxyethane in water is discussed in section 6.

5.1. Liquid Water

Liquid water is probably the most studied substance in both MD and MC simulations. One reason for this is that water is the most common solvent in chemistry and biology. Another reason is that liquid water has many anomalous properties. One anomaly

is that this small hydride is a liquid at room temperature and ambient pressure. This oddity may be explained by the fact that a water molecule can form hydrogen bonds with four other water molecules to form a tetrahedral network. Other well-known water anomalies are that its density maximum occurs at $4^{B}C$ and it has a large heat capacity, dielectric constant, and surface tension.[233,234] Obviously, substantial effort has been put into understanding these anomalous features of liquid water.[235−239]

The first MC and MD simulations of liquid water were carried out ca. 30 years ago,[240,241] and later explicit polarizabilities were included to describe the many-body effects and cooperativity occurring in liquid water.[211] A wealth of empirical and quantum chemical water potentials exist, but it is fair to state that no water potential is accurate and general enough to model all the properties of water in the condensed phases over a wide range of temperatures and pressures. Perhaps the most widely applicable potential thus far is the SPC potential obtained by Berendsen and co-workers,[178,241] which, despite its simplicity, has been applied extensively and with reasonable success.

Several MD simulations of liquid water have been performed using NEMO potentials.[14,61,85,243,244] The results of these simulations are generally in good agreement with the experimental radial distribution functions (RDF). Most notably, the second maximum in the oxygen−oxygen RDF, which is the signature of the tetrahedral structure in liquid water, is well reproduced. However, the NEMO simulations usually yield water structures that are slightly too organized compared to what is experimentally observed. It also has been shown that the oxygen−oxygen RDF is sensitive to the parametrization of the repulsion term.[61] Buontempo et al carried out a neutron diffraction study of liquid water at 573 K and compared the results to simulations using the NEMO model. They found excellent agreement between the two studies.[245] It should also be noted that the experimental RDFs for liquid water, which were obtained from neutron scattering experiments, have been recently revised.[246]

NEMO simulations have found the total internal energy of water to be -9.49 ± 0.09 kcal/mol[14] and -10.18 kcal/mol,[85] which are close to the experimental value of -9.92 kcal/mol, when the latter is corrected for quantum contributions (quoted in ref 178). The various contributions to the total energy are distributed as follows (with energies for the gas-phase dimer in parentheses): induction energy, -4.18 (-0.92) kcal/mol; dispersion energy, -3.96 (-1.52) kcal/mol; electrostatic energy, -12.66 (-7.31) kcal/mol; exchange−repulsion energy, $+11.31$ ($+4.79$) kcal/mol. The most dramatic difference between liquid water and the water dimer is the increased importance of the induction energy compared to the electrostatic energy that is observed for liquid water.

The calculated dipole moment of the water molecule in liquid water is 2.86 D.[14] This is close to the value of 2.95 D calculated in recent Car−Parrinello simulations[40,41] and slightly lower than the estimated experimental dipole moment of 3.09 D in ice.[49] The NEMO water model returns slower dynamic properties than those observed experimentally. The calculated diffusion coefficient is 1.3×10^{-5} cm^2 s^{-1} [14] or 1.0×10^{-5} cm^2 s^{-1} [85] compared to the experimental value of 2.3×10^{-5} cm^2 s^{-1}.[247] However, the center-of-mass velocity autocorrelation function from the simulation is in excellent agreement with the experimental results.[14]

The NEMO model also has been used to model liquid water at a hydrophobic wall.[243] It was found that the interactions with the wall are dominated by electrostatic interactions and that polarization plays a secondary role. The structural changes that occur at the wall are of relatively short range and only affect a few layers of water molecules. The NEMO model also has been adopted in an attempt to model the temperature-dependence of the density and especially the density maximum at 4 °C.[244] None of the applied water potentials were able to reproduce the density maximum, but it was demonstrated that only subtle changes to the potential at each temperature were required to reach the correct density. Obviously temperature-dependent potentials are not a viable approach, but they do demonstrate how sensitive the density is to the potential parameters. The NEMO water potential also has been used in combined quantum chemical and Monte Carlo studies.[230−232]

Recent developments in experimental techniques have provided more detailed and complex information about liquid water. For example, accurately modeling time-dependent fluorescence spectroscopy,[248] THz laser spectroscopy,[249−252] pump−probe spectroscopy,[253] and time-dependent neutron scattering[254,255] to obtain a more detailed understanding of these spectra will require the use of more accurate potentials as well as improved simulation techniques. Furthermore, studies have been carried out in the deep supercooled region of liquid water to better understand its anomalies.[256−258,238] It should be emphasized again that perturbation theory provides a theoretical background for the systematic development of more accurate potentials which are independent of experimental conditions.

5.2. Solvation of Ions in Water

Carignano et al. investigated the effect of ionic polarizability on the solvation of positive and negative ions in water.[259] They found that an increase in the polarizability leads to a larger electrical field at the ion which is due to the solvation shell shrinking around the ion and the probability increasing that the ion in the cage will be in an asymmetric location. The induced dipole moment in the first hydration shell was also investigated and found to be approximately the same size as in bulk water. This is due to the influences from the fields of the ion and the other water molecules in the hydration shell balancing. These results suggest that the surface activity of ions in water increases with their increasing polarizability, which is in agreement with experimental observations.

5.3. Aqueous Urea Solutions

NEMO potentials have been used to study aqueous urea solutions at different concentrations.[209,210] The

energy minimum of the urea dimers NEMO potential is in agreement with quantum chemical calculations and is much deeper than previously obtained empirical potentials.[61] The reason that the empirical potentials are too shallow is that the global minimum of the potential-energy surface is a cyclic arrangement of the urea dimer whereas the empirical potentials are parametrized from the linear structure adopted by crystalline urea. Since both types of dimer involve two hydrogen bonds, an isotropic and pairwise additive empirical potential would be expected to give similar interaction energies for the two dimers, and this is indeed the case.[260−262] However, with the NEMO potential, the minimum interaction energies are −22 kcal/mol for the cyclic dimer and −11 kcal/mol for the linear dimer.[61] This large difference between NEMO + empirical or cyclic + linear dimers intermolecular potentials leads to different results with respect to formation of the urea complex in water, and strong interactions between the urea molecules are found when using the NEMO potential.[210] Furthermore, it was found that the urea is well accommodated in the water structure, i.e., the water molecules in close proximity to the urea molecules maintain their liquid structure, and nine water molecules were found in the first hydration shell around the urea.[209] The results of the simulations were consistent with neutron scattering experiments,[263,264] and new neutron scattering experiments have been suggested that would definitely show the degree to which urea forms complexes in aqueous solutions.

5.4. Liquid Formaldehyde

Hermida-Ramón and Ríos constructed an intermolecular potential for the formaldehyde dimer by applying the Hayes−Stone intermolecular perturbation theory.[265] Their potential is in reasonably good agreement with the potential obtained from quantum chemical calculations for formaldehyde clusters. A simplified version of the potential was used in a subsequent a MD simulation. Their results showed that the dipole moment of formaldehyde is 10% higher in the liquid phase than in the gas phase. This increase in the dipole moment on going from the gas phase to the liquid phase is much smaller than that found for water.

5.5. Liquid Acetonitrile and Solvation of the Sodium Ion in Acetonitrile

Cabaleiro-Lago and Ríos studied liquid acetonitrile and the solvation of a Na^+ cation in liquid acetonitrile.[266] However, they used a somewhat different approach in constructing their force fields. The potential surfaces were fitted from MP2 calculations for bimolecular complexes with acetonitrile constrained such that the atomic charges reproduced the MEP and the molecular dipole moment. Atomic dipole polarizabilities determined according to the scheme by Stone[107] were added to the acetonitrile without altering the dimer's potential surfaces.

In the simulation of neat acetonitrile, a pronounced liquid structure was found only at short distances and the acetonitrile molecules were arranged in antiparallel orientations. It was noted that a pairwise additive model and a polarizable model give similar results for liquid acetonitrile. However, for the solvation of Na^+ in acetonitrile, the pairwise additive potential yielded a coordination number of 7 for the sodium ion whereas only six neighboring molecules were found when using the polarizable potential. This clearly demonstrates the importance of many-body interactions in ion solvation.

6. Intermolecular Potentials for Flexible Molecules

6.1. Inter- and Intramolecular Potentials

Discussions concerning the construction of intermolecular potentials (force fields) are usually restricted to rigid molecules. This limitation excludes flexible molecules such as proteins and polymers where the charge distribution is dependent on the molecule's conformation.[267] In many of the available force fields, the charge distribution is independent of the conformation.[31,32,268] However, if the aim is to construct accurate force fields, the charge distribution must be conformation-dependent. Unfortunately, taking the charge differences between different conformations into account is a nontrivial problem. One possible solution is to use local multicenter multipole expansions that depend on the dihedral angle.[269] It has been shown that the electrostatic potential around a flexible molecule is described very well by multipole moments as a function of the dihedral angle. Cumulative atomic multipole moments (CAMM) also have been successfully used to describe electrostatic interactions for flexible molecules.[270] However, these models do not address the problem of treating the intermolecular and intramolecular polarization effects at the same level, which must be taken into account in a realistic simulation of a flexible molecule in solution. Furthermore, the polarization equations for the inter- and intramolecular inductions should be solved simultaneously. One possible way to take these effects into account is outlined here. Usually, the change in the charge distribution of a flexible molecule, as it rotates around a dihedral angle, is related to the fact that the field originating from one part of the molecule and acting on other parts varies with the conformation. Thus, the change in the charge distribution is mainly inductive in origin. An intermolecular potential between 1,2-dimethoxyethane (DME, $CH_3-O-CH_2-CH_2-O-CH_3$) and water has been constructed as an example of the indicated methodology.[62] DME has in total 27 different conformations of 10 different types. The following notation will be used here: (*aaa*) describes the molecule when it adopts anti conformations around all three dihedral angles, (*aga*) describes the molecule when it adopts a gauche conformation around the C−C bond and anti conformations around the C−O bonds, (*aag*) describes the molecule when it adopts anti conformations around the C−C bond and one C−O bond and a gauche conformation around the other C−O bond.

Table 4. Comparison of the Dipole Moment for 1,2-Dimethoxyethane for Different Values of the C-C Dihedral Angle (both C-O bonds are in the anti conformation)[a]

	angle	μ_x	μ_y	μ_z
HF	60°	−0.397	0.200	0.0
corrected dipole moment	60°	−0.352	0.203	0.0
uncorrected dipole moment	60°	−0.324	0.187	0.0
HF	105°	−0.394	0.514	0.0
corrected dipole moment	105°	−0.390	0.508	0.0
uncorrected dipole moment	105°	−0.362	0.472	0.0

[a] Dipole moments are given in atomic units. The data are taken from Engkvist et al.[62]

A multicenter multipole expansion[70,71] was performed for the (*aaa*) conformer of DME. Electrostatic moments up to quadrupole moments were calculated at each atom and bond. Local polarizabilities in the uncoupled Hartree−Fock approach also were calculated at each atom and bond.[106] The dipole moment at each expansion center was regarded as consisting of two parts. One part originated from the local charge distribution around the expansion center (the local dipole moments), while the other part (the induced dipole moment) originated from the interaction between charges, local dipole moments, and quadrupoles located at other centers and the local polarizability at the expansion center. It is problematic to determine which expansion centers should interact with the polarizability of a given center. Obviously an expansion center should not interact with its neighboring expansion centers. In the case of DME, the molecule was divided into six groups and each group interacted with all other groups except for their neighboring groups.[62] To recover the charge distribution for a conformation, the charges, local dipole moments, and quadrupoles located at other centers were interacted with the local polarizability at the center of interest. The induced dipole moments then induced new dipole moments at other sites, in a manner analogous to the intermolecular induction treatment. It must be emphasized that this procedure is semiempirical in nature and its value originates from its capability to predict the total dipole moment for DME in different conformations. The idea behind this treatment of intramolecular induction effects is that a molecule's local polarizability can interact with the fields from charges, local dipole moments, and quadrupoles located at other centers as well as with charges, dipole moments and quadrupole moments from surrounding rigid molecules. Thus, inter- and intramolecular induction effects were treated at the same level in the simulation.

Table 4 demonstrates that the model outlined above accurately reproduces the total HF dipole moment for DME when the C−C bond is rotated. The model reproduces the total HF dipole moment better than when local electrostatic moments are used for the conformer with the lowest energy (the anti−anti−anti conformer).

6.2. 1,2-Dimethoxyethane in Water Solution

The new potential for DME−water was used in an MC simulation to investigate the temperature-dependence of the conformation distribution.[137] The reason for studying DME is that it is the smallest molecule that has a conformational behavior similar to poly(ethylene oxide) (PEO). It is well-known that while completely soluble in water at low temperatures, PEO loses its solubility at elevated temperatures. This process is normally termed clouding. Several different mechanisms have been suggested to explain why clouding occurs. Before discussing the results, we would like to briefly mention the problem of converging the conformation distribution for a flexible molecule in a molecular simulation. As extensively discussed in the literature, it is necessary to use either perturbation techniques or an umbrella potential to converge the probability distribution for the conformation. This issue has been addressed many times in connection with simulations of small flexible molecules.[271,272] The problem exists for molecules as small as butane in water, and it very rapidly becomes more difficult to reach convergence as the size of the molecule increases. This is because the number of conformations that a molecule can adopt grows as 3^n, where n is the number of dihedral angles in the molecule. DME in water also has been studied by other groups; however, these studies did not use either an umbrella potential or a perturbation technique to converge the probability distribution, which makes it impossible to compare their results with those of the study under discussion.[273,274] Simulations were performed at 298 and 398 K and 18 M steps were performed at each temperature. Even with this many steps it still was not possible to converge the conformation distribution at 298 K. The main results of the simulation are given in Table 5.

Table 5. Free Energy, Internal Energy, and Entropy for Each of the Most Important Conformations of DME at 398 K in Water and Their Free Energies in the Gas Phase

	{*aaa*}	{*aga*}	{*aag*}	{*aggN*}
$A^{(398)}_{\text{water}}$	0.0	0.2	−0.4	0.1
$U^{(398)}_{\text{water}}$	3.2	−0.4	−1.8	−1.0
$S^{(398)}_{\text{water}}$	8.1	−1.3	−3.5	−2.7
$A^{(398)}_{\text{gas phase}}$	0.0	−0.1	0.7	−0.9
$\delta Z^{(398)}/\delta T$	0.0102	−0.0011	−0.0058	−0.0030
$A^{(298)}_{\text{water}}$	0.0	−0.4	−0.9	(0.3)[b]
$A^{(398)}_{\text{gas phase}}$	0.0	0.1	0.9	−0.7
$U^{b(O)}_{\text{gas phase}}$	0.0	0.8	2.0	0.3

[a] The temperature derivative of the conformation distribution at 398 K and the free energy of the conformations at 298 K in water and in the gas phase. The gas-phase energies at 0 K. All energies are given in kcal/mol and entropies in cal/(mol*kelvin). The data are taken from Engkvist et. al.[137] [b] Uncertain due to poor convergence in the simulation.

It should be noted that several of the conformations have approximately the same energy. Thus, the results are sensitive to the potential used in the study. The intramolecular dihedral potential was calculated at the HF level with a London-type dispersion term added. It has been previously demonstrated that correlation effects influence the dihedral potential, such that the difference between the (*aaa*) and (*aga*) conformations decreases when correlation ef-

fects are included.[275] However, this problem mainly affects the absolute numbers obtained and not the conformational change as a function of temperature, which is the main interest here. Comparing the results from the two simulations and the temperature derivative of the partition function at 398 K shows that among the most populated conformers, only the anti−anti−anti (*aaa*) conformer increases its population with increasing temperature. Partitioning the energy into different contributions at 398 K reveals that the stability of the (*aga*), (*agg′*), and (*aag*) conformers compared to the (*aaa*) one originates primarily from the favorable water−water interactions obtained in the presence of these conformers, although the DME−water interaction does play a part.[137] Many-body effects on the conformation equilibrium seem to be small.[137] Of the most populated conformers, the nonpolar (*aaa*) is the only conformer that increases with increasing temperature. This is relevant with respect to understanding which mechanisms affect the clouding observed with the PEO−water system. An analysis indicates that (*aaa*) is entropically favored and other conformations are energetically stabilized by favorable water−water interactions. A closer analysis reveals that the simulation data are consistent with at least two of the suggested clouding mechanisms.[137]

7. Solvent Effects on Molecular Properties

Molecular properties such as frequency-dependent (hyper)polarizabilities and magnetic properties such as nuclear shielding constants and magnetizabilities are affected by the surrounding molecules in two main ways: the electronic structure is polarized and the geometry is altered. Solvent effects on molecular properties have been modeled in several different ways. Implicit models, where the molecule of interest is placed in a cavity within a dielectric medium then the molecular property of interest is calculated using regular quantum chemical methods, have been adopted extensively.[276−278] Explicit or semiexplicit models also have been employed. For example, molecular clusters have been generated in molecular simulations and the molecular property of interest for the central molecule in the cluster has been calculated.[279,280]

One method that is used to handle solvent properties is an extension of the perturbation approach discussed in section 2.1. In this method, a term that corresponds to an external perturbation, V_{ext}, is added to the Hamiltonian in eq 3

$$H = H_A + H_B + \lambda_1 V_{AB} + \lambda_2 V_{ext} \qquad (34)$$

As before, H_A and H_B are the Hamiltonians of the unperturbed molecules, V_{AB} denotes the interaction between molecules A and B, and λ_1 and λ_2 are order parameters. V_{ext} often denotes an interaction with an external electromagnetic field. The zeroth order in λ_2 gives the intermolecular interactions discussed in section 2.1, while the zeroth order in λ_1 can give molecular properties of the unperturbed molecules as defined in regular response or perturbation theory when V_{ext} is appropriately chosen. For nonzero orders in both λ_1 and λ_2, the contributions to the molecular properties arising from the intermolecular interactions are obtained. If electronic polarization is considered, the leading term arises from the electrostatic interactions[1]

$$\Omega_E = \Omega'_\alpha E_\alpha + \frac{1}{2}\Omega''_{\alpha\beta} E_\beta E_\alpha + \ldots + \frac{1}{3}\Omega'_{\alpha\beta} E_{\alpha\beta} + \frac{1}{6}\Omega''_{\alpha\beta,\gamma\delta} E_{\gamma\delta} E_{\alpha\beta} + \ldots \qquad (35)$$

where E_α is the electric field and $E_{\alpha\beta}$ is the electric field gradient. The various Ω^n's are the corresponding derivatives of the molecular property with respect to the perturbation. It should be noted that Ω^n is a response property for the unperturbed molecule and can be obtained using regular quantum chemical methods. However, in a distributed representation of the charge distribution, electric fields and field gradients are obtained at each atom, and therefore a distributed representation of Ω^n is also required. Induction contributions may be included in eq 35 by regarding E_α and $E_{\alpha\beta}$ as the total electric field and the field gradient, respectively, where both include contributions from the induced electric moments of the surrounding molecules. Additional contributions to intermolecular interactions arise from dispersion and exchange interactions.

This kind of perturbation approach has been used to calculate vibrational transition intensities for the HF dimer[281] and the chemical shifts of the water dimer[283,284] as well as for the Ar···HF and HF···CO_2 complexes.[28,284] However, the properties considered in these studies, that is, the gradient of the molecular dipole moment and the nuclear shielding constants, are trivially assigned to nuclei in the molecule. For a perturbation approach to chemical shifts, contributions from the anisotropy of the magnetizability of the neighboring molecules and dispersion interactions also are of importance,[285−288] even though pure electrostatic models have described chemical shifts with some success.[289−292]

The ensemble average of eq 7.35 can be obtained from MD or MC simulations of a molecular condensed phase. If the molecules are assumed to be rigid or if Ω^n is assumed to be independent of the molecular geometry, only ensemble averages of electric fields and field gradients have to be calculated.[282,293]

$$\langle\Omega_E\rangle = \Omega'_\alpha\langle E_\alpha\rangle + \frac{1}{2}\Omega''_{\alpha,\beta}\langle E_\beta E_\alpha\rangle + \ldots + \frac{1}{3}\Omega'_{\alpha\beta}\langle E_{\alpha\beta}\rangle + \frac{1}{6}\Omega''_{\alpha\beta,\gamma\delta}\langle E_{\gamma\delta} E_{\alpha\beta}\rangle + \ldots \qquad (36)$$

where $\langle\rangle$ denotes an ensemble average. The calculation of solvent effects on molecular properties therefore can be divided into two parts. (1) Quantum chemical calculations of molecular electric-field and electric field-gradient derivatives. Since the perturbation expansion is carried out at the limit of no perturbations, the quantum chemical calculations are performed for the unperturbed molecules. (2) MD or MC simulation calculations of the size of the perturbations arising from electric fields and field gradients at the atomic positions for liquids or solutions. It

should be emphasized that to obtain accurate electric fields and field gradients, the representation of the molecular charge distributions must also be accurate.

Thus, each part can be improved and investigated independently of the other part. This approach has been used to study chemical shifts[282,293] and the molecular geometry[294] of the water molecule in liquid water. Reasonable results were obtained for the temperature-dependent proton chemical shift, but problems still persist with the oxygen shift.[282,293]

Solvent effects were found to alter the geometry of a water molecule in liquid water, such that a 3.0 pm elongation of the O−H distance and a 2.0° increase in the bond angle were found at room temperature.[294] It was noted that the effect of the solvent on the bond angle was mainly due to dispersion interactions. Furthermore, the solvent effects decreased with increasing temperature. In a combined quantum chemical and classical MC study, an O−H bond length increase of 1.0 pm and a bond angle increase of 4.0° were calculated.[231] In contrast, a CP simulation yielded a calculated bond elongation of 1.9 pm and an increase in the bond angle of 1.1°.[41] These differences in the calculated O−H bond elongation are due to the differing treatments of the static electronic correlation. In the treatment where the molecular geometry was calculated using a multiconfigurational (SCF) method, a larger bond elongation was found.[294] That was to be expected since an MCSCF method generally gives a good description of phenomena such as bond breaking, which indicates that it gives a balanced description of a molecule at all geometries.[295] A direct comparison of the theoretical results with experiment is difficult since the experimental data largely consists of vibrational contributions.[294] However, all the theoretical results were within the limits of the experimental data.

To study solvent effects on molecular properties arising from the distortion of the molecular geometries, eq 35 must be extended to include geometric derivatives of the molecular properties as well as of the various Ω^n's. Furthermore, intramolecular motion cannot be treated by classical mechanics which requires that eq 36 be extended to also include vibrational averaging of the molecular properties.

8. Conclusions

The construction of intermolecular potentials based solely on quantum chemical calculations has made significant progress during recent years. In this review article, we have discussed the construction and application of intermolecular potentials based on intermolecular perturbation theory. At the long-range limit, the potential parameters can be calculated from monomer wave functions. The electrostatics are described using distributed multipole moments, and it is demonstrated that atomic charges alone are not sufficient to give an accurate description. In addition, intermolecular perturbation theory provides a convenient way to directly include distributed polarizabilities in methods such as molecular dynamics simulations. Thus, many-body effects can be included and have been demonstrated to be crucial to obtaining accurate descriptions of molecular clusters as well as of the solvation of ions and the adsorption of molecules or ions on surfaces. It is argued that atomic electrostatic moments and polarizability tensors cannot be regarded as transferable from one molecule to another. Exchange−repulsion is described using an isotropic or anisotropic exponential term and is related to the overlap of the wave functions of the interacting molecules. Dispersion interactions are described using at least a damped R^{-6} term and parameters obtained from molecular properties. In addition, extending the perturbation approach for intermolecular interactions to also include solvent effects on molecular properties is discussed. In conclusion, accurate potentials describe reality well and empirical potentials that are explicitly parametrized to reproduce experiments are, in many cases, not needed.

Despite its advantages, the approach discussed here should only be regarded as a starting point. So far, potentials based on intermolecular perturbation theory have been constructed for only a limited number of cases and no library of these types of potentials exists. Furthermore, the accuracy of the potentials has to be improved in order to keep up with the rapid development of experimental techniques. For instance, no water potential constructed for simulations of the liquid has yet been able to predict the vibration−rotation spectra observed for the water dimer.[167] Fortunately intermolecular perturbation theory is especially well suited to improvements. Since the interaction energy is formally partitioned into different energy contributions and the parameters are calculated from the molecular wave function, each part of the force field can be improved independently of the other parts. For example, the accuracy could be improved for clusters by including three-body corrections to the dispersion and exchange−repulsion terms.

9. References

(1) Buckingham, A. D. *Adv. Chem. Phys.* **1967**, *12*, 107−143.
(2) Müller-Dethlefs, K.; Hobza, P. *Chem. Rev.* **2000**, *100*, 143.
(3) Buckingham, A. D. In *Intermolecular Interactions from Diatomics to Biopolymers*; Pullman, B., Ed.; Wiley: Chichester, 1978; pp 1−67.
(4) Margenau, M.; Kestner, N. R. *Theory of Intermolecular forces*; Pergamon: Oxford, 1969.
(5) Claverie, P. In *Intermolecular Interactions: from Diatomics to Biopolymers*; Pullman, B., Ed.; Wiley: 1978; pp 69−305.
(6) Maitland, G. C.; Rigby, M.; Smith, E. B.; Wakeham, W. A. *Intermolecular Forces. Their Origin and Determination*; Oxford University Press: Oxford, 1981.
(7) Jeziorski, B.; Moszynski, R.; Szalewicz, K. *Chem. Rev.* **1994**, *94*, 1887.
(8) Stone, A. J. *The Theory of Intermolecular forces*; Clarendon: Oxford, 1996.
(9) Price, S. L. *Rev. Comput. Chem.* **2000**, *14*, 225.
(10) Dykstra, C. E. *Theor. Chem. Acc.* **2000**, *103*, 278.
(11) Allen, M. P.; Tildesey, D. J. *Computer Simulations of Liquids*; Oxford University Press: Oxford, 1987.
(12) Frenkel, D.; Smit, B. *Understanding Molecular Simulation*; Academic Press: San Diego, 1996.
(13) Wallqvist, A.; Karlström, G. *Chem. Scr.* **1989**, *29A* 131.
(14) Wallqvist, A.; Ahlström, P.; Karlström, G. *J. Phys. Chem.* **1990**, *94*, 1649; **1991**, *95*, 4922.
(15) Åstrand, P.-O. Hydrogen bonding as described with perturbation theory. Thesis, University of Lund, 1994.
(16) Engkvist, O. Flexible molecular systems studied by quantum chemistry and statistical mechanics. Thesis, University of Lund, 1997.
(17) Brdarski, S. Modelling of intra- and intermolecular potentials. Thesis, University of Lund, 1999.

(18) Hobza, P.; Zahradnik, R. *Intermolecular Complexes*; Elsevier: Amsterdam, 1988.
(19) Hobza, P. *Ann. Rep. Prog. Phys. Chem.* **1997**, *93*, 257−287.
(20) Matsuoka, O.; Clementi, E.; Yoshimine, M. *J. Chem. Phys.* **1976**, *64*, 1351.
(21) Clementi, E.; Cavallone, F.; Scordamaglia, R. *J. Am. Chem. Soc.* **1977**, *99*, 5531−5557.
(22) Scordamaglia, R.; Cavallone, F.; Clementi, E. *J. Am. Chem. Soc.* **1977**, *99*, 5545.
(23) Sordo, J. A.; Probst, M.; Corongiu, G.; Chin, S.; Clementi, E. *J. Am. Chem. Soc.* **1987**, *109*, 1702−1708.
(24) Niesar, U.; Corongiu, G.; Huang, M.-J.; Dupuis, M.; Clementi, E. *Int. J. Quantum Chem. Quantum Chem. Symp.* **1989**, *23*, 421.
(25) Karpfen, A.; Bunker, P. R.; Jensen, P. *Chem. Phys.* **1991**, *149*, 299.
(26) Klopper, W.; Quack, M.; Suhm, M. A. *J. Chem. Phys.* **1998**, *108*, 10096.
(27) Dang, L. X. *J. Phys. Chem. B* **1997**, *101*, 3413.
(28) Dang, L. X. *J. Chem. Phys.* **1999**, *110*, 10113.
(29) Tuma, C.; Boese, A. D.; Handy, N. C. *PCCP* **1999**, *1*, 3939.
(30) Weiner, S. J.; Kollman, P. A.; Case, D. A.; Singh, U. C.; Ghio, C.; Alagona, G.; Profeta, S.; Weiner, P. *J. Am. Chem. Soc.* **1984**, *106*, 765−784.
(31) Brooks, B. R.; Bruccoleri, R. E.; Olafson, B. D.; States, D. J.; Swaminathan, S.; Karplus, M. *J. Comput. Chem.* **1983**, *4*, 187−217.
(32) Hermans, J.; Berendsen, H. J. C.; van Gunsteren, W. F.; Postma, J. P. M. *Biopolymers* **1984**, *23*, 1513−1518.
(33) Jorgensen, W. L.; Tirado-Rives, J. *J. Am. Chem. Soc.* **1988**, *110*, 1657−1666.
(34) Brodsky, A. *Chem. Phys. Lett.* **1996**, *261*, 563.
(35) Dykstra, C. E. *J. Am. Chem. Soc.* **1989**, *111*, 6168−6174.
(36) Dykstra, C. E. *J. Am. Chem. Soc.* **1990**, *112*, 7540−7545.
(37) Augspurger, J. D.; Dykstra, C. E.; Zwier, T. S. *J. Phys. Chem.* **1992**, *96*, 7252−7257.
(38) Dykstra, C. E. *Chem. Rev.* **1993**, *93*, 2339.
(39) Car, R.; Parrinello, M. *Phys. Rev. Lett.* **1985**, *55*, 2471.
(40) Silvestrelli, P. L.; Parrinello, M. *Phys. Rev. Lett.* **1999**, *82*, 3308.
(41) Silvestrelli, P. L.; Parrinello, M. *J. Chem. Phys.* **1999**, *111*, 3572.
(42) Marx, D.; Tuckerman, M. E.; Hutter, J.; Parrinello, M. *Nature* **1999**, *397*, 601.
(43) Jeffrey, G. A. *An introduction to hydrogen bonding*; Oxford University Press: Oxford, 1997.
(44) Naray-Szabo, G.; Ferenczy, G. G. *Chem. Rev.* **1995**, *95*, 829.
(45) Warshel, A.; Levitt, M. *J. Mol. Biol.* **1976**, *103*, 227−249.
(46) Warshel, A.; Åqvist, J. *Annu. Rev. Biophys. Biophys. Chem.* **1991**, *20*, 267−298.
(47) Buckingham, A. D.; Fowler, P. W. *J. Chem. Phys.* **1983**, *79*, 6426−6429.
(48) Buckingham, A. D.; Fowler, P. W. *Can. J. Chem.* **1985**, *63*, 2018−2025.
(49) Batista, E. R.; Xantheas, S. S.; Jonsson, H. *J. Chem. Phys.* **1998**, *109*, 4546.
(50) Pitzer, K. S. *Adv. Chem. Phys.* **1959**, *2*, 59−83.
(51) van Lenthe, J. H.; van Duijneveldt-van de Rijdt, J. G. C. M.; van Duijneveldt, F. B. *Adv. Chem. Phys.* **1987**, *69*, 521−566.
(52) Rullman, J. A. C.; van Duijnen, P. T. *Rep. Mol. Theor.* **1990**, *1*, 1−21.
(53) Hayes, I. C.; Stone, A. J. *Mol. Phys.* **1984**, *53*, 83−105.
(54) Chalasinski, G.; Szczesniak, M. M. *Chem. Rev.* **1994**, *94*, 1723.
(55) Claverie, P. *Int. J. Quantum Chem.* **1971**, *5*, 273.
(56) Morgan III, J. D.; Simon, B. *Int. J. Quantum Chem.* **1980**, *17*, 1143.
(57) Amos, A. T.; Musher, J. I. *Chem. Phys. Lett.* **1969**, *3*, 721.
(58) Adams, W. H. *Chem. Phys. Lett.* **1994**, *229*, 472−480.
(59) Jeziorski, B.; Kobs, W. In *Molecular interactions*; Ratajczak, H.; Orville-Thomas, W. J., Eds.; Wiley: New York, 1982; Vol. 3.
(60) Stone, A. J. In *Advances in biomolecular simulations*; Lavery, R., Rivail, J.-L., Smith, J., Eds. American Institute of Physics: New York, 1991; pp 3−19.
(61) Åstrand, P.-O.; Wallqvist, A.; Karlström, G. *J. Chem. Phys.* **1994**, *100*, 1262.
(62) Engkvist, O.; Åstrand, P.-O.; Karlström, G. *J. Phys. Chem.* **1996**, *100*, 6950.
(63) Millot, C.; Stone, A. J. *Mol. Phys.* **1992**, *77*, 439−462.
(64) Millot, C.; Soetens, J.-C.; Martins Costa, M. T. C.; Hodges, M. P.; Stone, A. J. *J. Phys. Chem. A* **1998**, *102*, 754−770.
(65) Hodges, M. P.; Stone, A. J.; Cabaleiro Lago, E. *J. Phys. Chem. A* **1998**, *102*, 2455−2465.
(66) Wheatley, R. J. *Mol. Phys.* **1996**, *87*, 1083.
(67) Gray, C. G.; Gubbins, K. E. *Theory of Molecular Fluids*; Clarendon Press: Oxford, 1984; Vol. 1 (Fundamentals).
(68) Cioslowski, J. *Phys. Rev. Lett.* **1989**, *62*, 1469−1471.
(69) Stone, A. J. *Chem. Phys. Lett.* **1993**, *211*, 101−109.
(70) Karlström, G. On the evaluation of intermolecular potentials. In *Proceedings of the 5th Seminar on Computational Methods in Quantum Chemistry*; van Duijnen, W. C., Nieuwpoort, P. T., Eds.; p 353, Laboratory of Chemical Physics: University of Gronningen, Nijenborgh 16, 9747 AG Gronningen, The Netherlands, 1981. Max-Plank-Institut für Physik und Astrophysik; Institut für Astrophysik, Karl-Schwarzschild-Strasse 1, 857 40 Garching bei München, Deutschland.
(71) Andersson, M.; Karlström, G. *J. Phys. Chem.* **1985**, *89*, 4957.
(72) Stone, A. J. *Chem. Phys. Lett.* **1981**, *83*, 233.
(73) Port, G. N. J.; Pullman, A. *FEBS Lett.* **1973**, *31*, 70−74.
(74) Rein, R. *Adv. Quantum Chem.* **1973**, *7*, 335.
(75) Sokalski, W. A.; Poirier, R. A. *Chem. Phys. Lett.* **1983**, *98*, 86.
(76) Vigne-Mader, F.; Claverie, P. *J. Chem. Phys.* **1988**, *88*, 4934.
(77) Stone, A. J.; Alderton, M. *Mol. Phys.* **1985**, *56*, 1047.
(78) Thole, B. T.; van Duijnen, P. T. *Theor. Chim. Acta* **1983**, *63*, 209−221.
(79) Wheatley, R. J. *Chem. Phys. Lett.* **1993**, *208*, 159.
(80) Jansen, G.; Hättig, C.; Hess, B. A.; Angyan, J. G. *Mol. Phys.* **1996**, *88*, 595.
(81) Chipot, C.; Angyan, J. G.; Millot, C. *Mol. Phys.* **1998**, *94*, 881.
(82) Bellido, M. N.; Rullman, J. A. C. *Int. J. Quantum Chem.* **1989**, *10*, 479.
(83) Li, J.; Zhu, T.; Cramer, C. J.; Truhlar, D. G. *J. Phys. Chem. A* **1998**, *102*, 1820−1831.
(84) Mulliken, R. S. *J. Chem. Phys.* **1955**, *23*, 1833.
(85) Åstrand, P.-O.; Linse, P.; Karlström, G. *Chem. Phys.* **1995**, *191*, 195.
(86) Brdarski, S.; Karlström, G. *J. Phys. Chem. A* **1998**, *102*, 8182−8192.
(87) Momany, F. A. *J. Phys. Chem.* **1978**, *82*, 592.
(88) Cox, S. R.; Williams, D. E. *J. Comput. Chem.* **1981**, *2*, 304−323.
(89) Singh, U. C.; Kollman, P. A. *J. Comput. Chem.* **1984**, *5*, 129−145.
(90) Ferenczy, G. G. *J. Comput. Chem.* **1991**, *12*, 913.
(91) Winn, P. J.; Ferenczy, G. G.; Reynolds, C. A. *J. Phys. Chem. A* **1997**, *101*, 5437.
(92) Ferenczy, G. G.; Winn, P. J.; Reynolds, C. A. *J. Phys. Chem. A* **1997**, *101*, 5446.
(93) Wiberg, K. B.; Rablen, P. R. *J. Comput. Chem.* **1993**, *14*, 1504−1518.
(94) Dixon, R. W.; Kollman, P. A. *J. Comput. Chem.* **1997**, *18*, 1632.
(95) Hunter, C. A.; Sanders, J. K. M. *J. Am. Chem. Soc.* **1990**, *112*, 5525−5534.
(96) Helgaker, T. U.; Jensen, H. J. A.; Jørgensen, P. *J. Chem. Phys.* **1986**, *84*, 6280.
(97) Cioslowski, J. *J. Am. Chem. Soc.* **1989**, *111*, 8333−8336.
(98) Cioslowski, J.; Hay, P. J.; Ritchie, J. P. *J. Phys. Chem.* **1990**, *94*, 148−151.
(99) Cioslowski, J.; Hamilton, T.; Scuseria, G.; Jr, B. A. H.; Hu, J.; Schaad, L. J.; Dupuis, M. *J. Am. Chem. Soc.* **1990**, *112*, 4183−4186.
(100) de Proft, F.; Martin, J. M. L.; Geerlings, P. *Chem. Phys. Lett.* **1996**, *250*, 393−401.
(101) Åstrand, P.-O.; Ruud, K.; Mikkelsen, K. V.; Helgaker, T. *J. Phys. Chem. A* **1998**, *102*, 7686−7691.
(102) Dinur, U.; Hagler, A. T. *J. Chem. Phys.* **1989**, *91*, 2949−2958.
(103) Dinur, U.; Hagler, A. T. *J. Chem. Phys.* **1989**, *91*, 2959−2970.
(104) Dinur, U. *J. Phys. Chem.* **1990**, *94*, 5669−5671.
(105) Dinur, U.; Hagler, A. T. *J. Comput. Chem.* **1995**, *16*, 154−170.
(106) Karlström, G. *Theor. Chim. Acta* **1982**, *60*, 535.
(107) Stone, A. J. *Mol. Phys.* **1985**, *56*, 1065.
(108) Le Sueur, C. R.; Stone, A. J. *Mol. Phys.* **1993**, *78*, 1267.
(109) Le Sueur, C. R.; Stone, A. J. *Mol. Phys.* **1994**, *83*, 293.
(110) Angyan, J. G.; Jansen, G.; Loos, M.; Hättig, C.; Hess, B. *Chem. Phys. Lett.* **1994**, *219*, 267.
(111) Stone, A. J.; Hättig, C.; Jansen, G.; Angyan, J. G. *Mol. Phys.* **1996**, *89*, 595.
(112) Hättig, C.; Jansen, G.; Hess, B. A.; Angyan, J. G. *Can. J. Chem.* **1996**, *74*, 976.
(113) van Duijnen, P. T.; Swart, M. *J. Phys. Chem. A* **1998**, *102*, 2399.
(114) Winn, P. J.; Ferenczy, G. G.; Reynolds, C. A. *J. Comput. Chem.* **1999**, *20*, 704.
(115) Celebi, N.; Angyan, J. G.; Dehez, F.; Millot, C.; Chipot, C. *J. Chem. Phys.* **2000**, *112*, 2709.
(116) Åstrand, P.-O.; Karlström, G. *Mol. Phys.* **1992**, *77*, 143−155.
(117) Banks, J. L.; Kaminski, G. A.; Zhou, R.; Mainz, D. T.; Berne, B. J.; Friesner, R. A. *J. Chem. Phys.* **1999**, *110*, 741.
(118) Stern, H. A.; Kaminski, G. A.; Banks, J. L.; Zhou, R.; Berne, B. J.; Friesner, R. A. *J. Phys. Chem. B* **1999**, *103*, 4730.
(119) Boettcher, C. J. F. *Theory of Electric Polarization*, 2nd ed.; Elsevier: Amsterdam, 1973; Vol. 1.
(120) Stone, A. J. *Chem. Phys. Lett.* **1989**, *155*, 102.
(121) Price, S. L. *Chem. Phys. Lett.* **1985**, *114*, 359−364.
(122) Price, S. L.; Stone, A. J. *J. Chem. Soc. Faraday Trans.* **1992**, *88*, 1755−1763.
(123) Silberstein, L. *Philos. Mag.* **1917**, *33*, 521−533.
(124) Applequist, J.; Carl, J. R.; Fung, K.-F. *J. Am. Chem. Soc.* **1972**, *94*, 2952−2960.
(125) Applequist, J. *Acc. Chem. Res.* **1977**, *10*, 79−85.
(126) Thole, B. T. *Chem. Phys.* **1981**, *59*, 341−350.
(127) Olson, M. L.; Sundberg, K. R. *J. Chem. Phys.* **1978**, *69*, 5400−5404.
(128) Applequist, J. *J. Phys. Chem.* **1993**, *97*, 6016−6023.

(129) Tang, K. T.; Toennis, J. P. *J. Chem. Phys.* **1984**, *80*, 3726.
(130) McDowell, S. A. C.; Meath, W. J. *Can. J. Chem.* **1998**, *76*, 483.
(131) Wormer, P. E. S.; Hettema, H. *J. Chem. Phys.* **1992**, *97*, 5592.
(132) Jansen, A. R.; A., A. R. *J. Chem. Phys.* **1997**, *107*, 914.
(133) Stone, A. J.; Tong, C. S. *Chem. Phys.* **1989**, *137*, 121.
(134) Hättig, C.; Jansen, G.; Hess, B. A.; Angyan, J. G. *Mol. Phys.* **1997**, *91*, 145.
(135) Hodges, M. P.; Stone, A. J. *Mol. Phys.* **2000**, *98*, 275.
(136) Unsöld, A. *Z. Physik* **1927**, *43*, 563.
(137) Engkvist, O.; Karlström, G. *J. Chem. Phys.* **1997**, *106*, 2411.
(138) Boys, S. F.; Bernardi, F. *Mol. Phys.* **1970**, *19*, 553−566.
(139) Hermida-Ramón, J. M.; Engkvist, O.; Karlström, G. *J. Comput. Chem.* **1998**, *19*, 1816−1825.
(140) Stone, A. J.; Tong, C. S. *J. Comput. Chem.* **1994**, *15*, 1377.
(141) Fraschini, E.; Stone, A. J. *J. Comput. Chem.* **1998**, *19*, 847.
(142) Wheatley, R. J.; Price, S. L. *Mol. Phys.* **1990**, *69*, 507−533.
(143) Nobeli, I.; Price, S. L.; Wheatley, R. J. *Mol. Phys.* **1998**, *95*, 525.
(144) Mas, E. M.; Szalewicz, K.; Bukowski, R.; Jeziorski, B. *J. Chem. Phys.* **1997**, *107*, 4207.
(145) Fellers, R. S.; Leforestier, C.; Braly, L. B.; Brown, M. G.; Saykally, R. J. *Science* **1999**, *284*, 945−948.
(146) Meuwly, M.; Hutson, J. M. *J. Chem. Phys.* **1997**, *110*, 8338.
(147) Elrod, M. J.; Saykally, R. J. *Chem. Rev.* **1994**, *94*, 1975−1997.
(148) Axilrod, P. M.; Teller, E. *J. Chem. Phys.* **1943**, *11*, 299−300.
(149) Chalasinski, G.; Szczesniak, M. M.; Kendall, R. A. *J. Chem. Phys.* **1994**, *101*, 8860.
(150) Wells, B. H.; Wilson, S. *Mol. Phys.* **1986**, *57*, 21−32.
(151) Chalasinski, G.; Rak, J.; Szczesniak, M. M.; Cybulski, S. M. *J. Chem. Phys.* **1997**, *106*, 3301.
(152) Cooper, A. R.; Hutson, J. M. *J. Chem. Phys.* **1993**, *98*, 5337−5351.
(153) Ernesti, A.; Hutson, J. M. *J. Chem. Soc., Faraday Discuss.* **1994**, *97*, 119−129.
(154) Meredith, A. W.; Nordholm, S. *Chem. Phys.* **1997**, *220*, 63.
(155) Meredith, A. W.; Stone, A. J. *J. Phys. Chem. A* **1998**, *102*, 434−445.
(156) Cabaleiro-Lago, E. M.; Rios, M. A. *J. Chem. Phys.* **1999**, *110*, 6782.
(157) Cabaleiro-Lago, E. M.; Rios, M. A. *J. Chem. Phys.* **1998**, *109*, 8398.
(158) Cabaleiro-Lago, E. M.; Rios, M. A. *J. Phys. Chem. A* **1997**, *101*, 8327.
(159) Hodges, M. P.; Stone, A. J. *J. Chem. Phys.* **1999**, *110*, 6766.
(160) Engdahl, A.; Nelander, B.; Åstrand, P.-O. *J. Chem. Phys.* **1993**, *99*, 4894.
(161) Åstrand, P.-O.; Karlström, G.; Engdahl, A.; Nelander, B. *J. Chem. Phys.* **1995**, *102*, 3534.
(162) Stone, A. J.; Tantirungrotechai, Y.; Buckingham, A. D. *PCCP* **2000**, *2*, 429.
(163) Stone, A. J.; Dullweber, A.; Engkvist, O.; Hodges, M. P.; Meredith, A. W.; Popelier, P. L. A.; Wales, D. J. *Orient: a program for studying interactions between molecules*, version 4.0; University of Cambridge, Cambridge, 2000.
(164) Popelier, P. L. A.; Stone, A. J. *Mol. Phys.* **1994**, *82*, 411−425; **1995**, *84*, 811.
(165) Milet, A.; Mosszynski, R.; Wormer, P. E. S.; van der Avoird, A. *J. Phys. Chem. A* **1999**, *103*, 6811−6819.
(166) Cruzan, J. D.; Braly, L. B.; Liu, K.; Brown, M. G.; Loeser, J. G.; Saykally, R. J. *Science*, **1996**, *271*, 59.
(167) Fellers, R. S.; Braly, L. B.; Saykally, R. J.; Leforestier, C. *J. Chem. Phys.* **1999**, *110*, 6306.
(168) Engkvist, O.; Forsberg, N.; Schütz, M.; Karlström, G. *Mol. Phys.* **1997**, *90*, 277.
(169) Hodges, M. P.; Stone, A. J.; Xantheas, S. S. *J. Phys. Chem. A* **1997**, *101*, 9163−9168.
(170) Alkorta, I.; Bachs, M.; Perez, J. J. *Chem. Phys. Lett.* **1994**, *224*, 160−165.
(171) Chalasinski, G.; Szczesniak, M. M.; Cieplak, P.; Scheiner, S. *J. Chem. Phys.* **1991**, *94*, 2873.
(172) Schütz, M.; Bürgi, T.; Leutwyler, S.; Bürgi, H. B. *J. Chem. Phys.* **1993**, *99*, 5228. (E) **1994**, 100, 1780.
(173) van Duijneveldt-van de Rijdt, J. G. C. M.; van Duijneveldt, F. B. *Chem. Phys. Lett.* **1995**, *237*, 560.
(174) Klopper, W.; Schütz, M.; Lüthi, H. P.; Leutwyler, S. *J. Chem. Phys.* **1995**, *103*, 1085.
(175) van Duijneveldt-van de Rijdt, J. G. C. M.; van Duijneveldt, F. B. *Chem. Phys.* **1993**, *175*, 271.
(176) Fowler, J. E.; Schaefer III, H. F. *J. Am. Chem. Soc.* **1995**, *117*, 446.
(177) Schütz, M.; Klopper, W.; Lüthi, H. P. *J. Chem. Phys.* **1995**, *103*, 6115.
(178) Berendsen, H. J. C.; Grigera, J. R.; Straatsma, T. P. *J. Phys. Chem.* **1987**, *91*, 6269−6271.
(179) Jorgensen, W. L.; Chandrasekhar, J.; Madura, J. D.; Impey, R. W.; Klein, M. L. *J. Chem. Phys.* **1983**, *79*, 926−935.
(180) Owicki, J. C.; Shipman, L. L.; Scheraga, H. A. *J. Phys. Chem.* **1975**, *79*, 1794.
(181) Bürgi, T.; Graf, S.; Leutwyler, S.; Klopper, W. *J. Chem. Phys.* **1995**, *103*, 1077.
(182) Hartke, B.; Schütz, M.; Werner, H.-J. *Chem. Phys.* **1998**, *239*, 561−572.
(183) Wales, D. J.; Walsh, T. R. *J. Chem. Phys.* **1996**, *105*, 6957−6971.
(184) Spirko, V.; Engkvist, O.; Soldan, P.; Selzle, H.; Schlag, E. W.; Hobza, P. *J. Chem. Phys.* **1999**, *111*, 572−582.
(185) Hobza, P.; Selzle, H.; Schlag, E. W. *J. Phys. Chem.* **1996**, *100*, 18790.
(186) Karlström, G.; Linse, P.; Wallqvist, A.; Jönsson, B. *J. Am. Chem. Soc.* **1983**, *105*, 3777.
(187) Engkvist, O.; Selzle, H.; Schlag, E. W.; Hobza, P. *J. Chem. Phys.* **1999**, *110*, 5758−5762.
(188) de Meijere, A.; Huisken, F. *J. Chem. Phys.* **1990**, *92*, 5826.
(189) van der Waal, B. W. *Chem. Phys. Lett.* **1986**, *123*, 69.
(190) Peterson, K. A.; Dunning, T. H. *J. Chem. Phys.* **1995**, *102*, 2032.
(191) Howard, B. J.; Dyke, T. R.; Klemperer, W. *J. Chem. Phys.* **1984**, *81*, 5417.
(192) Cabaleiro-Lago, E. M.; Rios, M. A. *J. Chem. Phys.* **1998**, *108*, 3598.
(193) King, B. F.; Weinhold, F. *J. Chem. Phys.* **1995**, *103*, 333.
(194) Stone, A. J.; Buckingham, A. D.; Fowler, P. W. *J. Chem. Phys.* **1997**, *107*, 1030.
(195) Engkvist, O.; Stone, A. J. *Surface Sci.* **1999**, *437*, 239−248.
(196) Engkvist, O.; Stone, A. J. *J. Chem. Phys.* **1999**, *110*, 12089−12096.
(197) Picaud, S.; Hoang, P. N. M.; Girardet, C.; Meredith, A.; Stone, A. J. *Surface Sci.* **1993**, *294*, 149−160.
(198) Meredith, A. W.; Stone, A. J. *J. Chem. Phys.* **1996**, *104*, 3058−3070.
(199) Berg, O.; Ewing, G. E.; Meredith, A. W.; Stone, A. J. *J. Chem. Phys.* **1996**, *104*, 6843−6855.
(200) Fowler, P.; Madden, P. A. *Phys. Rev. A* **1984**, *29*, 1035−1042.
(201) Estel, J.; Hoinkes, H.; Kaarmann, H.; Nahr, H.; Wilsch, H. *Surface Sci.* **1975**, *54*, 393−418.
(202) Bruch, L. W.; Glebov, A.; Toennies, J. P.; Weiss, H. *J. Chem. Phys.* **1995**, *103*, 5109−5120.
(203) Fölsch, S.; Henzler, M. *Surface Sci.* **1991**, *247*, 269−273.
(204) Wassermann, B.; Mirbt, S.; Reif, J.; Zink, J. C.; Mattias, E. *J. Chem. Phys.* **1993**, *98*, 10049−10060.
(205) Heidberg, J.; Redlich, B.; Wetter, D. *Ber. Bunsen-Ges. Phys. Chem.* **1995**, *99*, 1333−1337.
(206) Richardson, H. H.; Baumann, C.; Ewing, G. E. *Surface Sci.* **1987**, *185*, 15.
(207) Heidberg, J.; Kampschoff, E.; Suhren, M. *J. Chem. Phys.* **1991**, *95*, 9408.
(208) Linse, P.; Wallqvist, A.; Åstrand, P.-O.; Nymand, T. M.; Lobaskin, V. *MOLSIM 2.8.0*; Lund University: Sweden, 1999.
(209) Åstrand, P.-O.; Wallqvist, A.; Karlström, G.; Linse, P. *J. Chem. Phys.* **1991**, *95*, 6395−6396.
(210) Åstrand, P.-O.; Wallqvist, A.; Karlström, G. *J. Phys. Chem.* **1994**, *98*, 8224−8233.
(211) Barnes, P.; Finney, J. L.; Nicholas, J. D.; Quinn, J. E. *Nature* **1979**, *282*, 459−464.
(212) Sprik, M.; Klein, M. L. *J. Chem. Phys.* **1988**, *89*, 7556−7560.
(213) Sprik, M.; Klein, M. L.; Watanabe, K. *J. Phys. Chem.* **1990**, *94*, 6483−6488.
(214) Ahlström, P.; Wallqvist, A.; Engström, S.; Jönsson, B. *Mol. Phys.* **1989**, *68*, 563−581.
(215) Rick, S. W.; Stuart, S. J.; Berne, B. J. *J. Chem. Phys.* **1994**, *101*, 6141−6156.
(216) Ruocco, G.; Sampoli, M. *Mol. Phys.* **1994**, *82*, 875−886.
(217) Vesely, F. J. *J. Comput. Phys.* **1977**, *24*, 361−371.
(218) Price, S. L.; Stone, A. J.; Alderton, M. *Mol. Phys.* **1984**, *52*, 987−1001.
(219) Rodger, P. M.; Stone, A. J.; Tildesley, D. J. *J. Chem. Soc., Faraday Trans. 2* **1987**, *83*, 1689−1702.
(220) Rodger, P. M.; Stone, A. J.; Tildesley, D. J. *Mol. Phys.* **1988**, *63*, 173−188.
(221) Rodger, P. M.; Stone, A. J.; Tildesley, D. J. *Chem. Phys. Lett.* **1988**, *145*, 365−370.
(222) Yashonath, S.; Price, S. L.; McDonald, I. R. *Mol. Phys.* **1988**, *64*, 361−376.
(223) Rodger, P. M. *Mol. Phys.* **1992**, *76*, 1385−1396.
(224) Nymand, T. M.; Linse, P. *J. Chem. Phys.* **2000**, *112*, 6152.
(225) Nymand, T. M.; Linse, P. *J. Chem. Phys.* **2000**, *112*, 6386.
(226) Zhu, S.-B.; Singh, S.; Robinson, G. W. *J. Chem. Phys.* **1991**, *95*, 2791.
(227) Zhu, S.-B.; Wong, C. F. *J. Phys. Chem.* **1994**, *98*, 4695.
(228) Soetens, J.-C.; Millot, C. *Chem. Phys. Lett.* **1995**, *235*, 22−30.
(229) Remler, D. K.; Madden, P. A. *Mol. Phys.* **1990**, *70*, 921−966.
(230) Moriarty, N. W.; Karlström, G. *J. Phys. Chem.* **1996**, *100*, 17791−17796.
(231) Moriarty, N. W.; Karlström, G. *J. Chem. Phys.* **1997**, *106*, 6470−6474.
(232) Moriarty, N. W.; Karlström, G. *Chem. Phys. Lett.* **1997**, *279*, 372−376.
(233) Eisenberg, D.; Kauzmann, W. *The structure and properties of water*; Clarendon: Oxford, 1969.
(234) Franks, F., Ed. *Water: A comprehensive treatise*; Plenum Press: New York, 1972−82; Vols. 1−7.

(235) Bassez, M.-P.; Lee, J.; Robinson, G. W. *J. Phys. Chem.* **1987**, *91*, 5818−5825.
(236) Ohmine, I. *J. Phys. Chem.* **1995**, *99*, 6767−6776.
(237) Ohmine, I.; Saito, S. *Acc. Chem. Res.* **1999**, *32*, 741−749. 825(E).
(238) Mishima, O.; Stanley, H. E. *Nature* **1998**, *396*, 329−335.
(239) Chialvo, A. A.; Cummings, P. T. *Adv. Chem. Phys.* **1999**, *109*, 115−205.
(240) Barker, J. A.; Watts, R. O. *Chem. Phys. Lett.* **1969**, *3*, 144−145.
(241) Rahman, A.; Stillinger, F. H. *J. Chem. Phys.* **1971**, *55*, 3336.
(242) Berendsen, H. J. C.; Postma, J. P. M.; van Gunsteren, W. F.; Hermans, J. In *Intermolecular forces*; Pullmann, B., Ed.; Reidel: Dordrecht, 1981; p 331.
(243) Wallqvist, A. *Chem. Phys. Lett.* **1990**, *165*, 437−442.
(244) Wallqvist, A.; Åstrand, P. *J. Chem. Phys.* **1994**, *102*, 6559−6565.
(245) Buontempo, U.; Postorino, P.; Ricci, M. A.; Soper, A. K. *Europhys. Lett.* **1992**, *19*, 385−389.
(246) Soper, A. K.; Bruni, F.; Ricci, M. A. *J. Chem. Phys.* **1997**, *106*, 247−254.
(247) Krynicki, K.; Green, C. D.; Savyer, D. W. *Discuss. Faraday Soc.* **1978**, *66*, 199.
(248) Jimenez, R.; Fleming, G. R.; Kumar, P. V.; Maroncelli, M. *Science* **1994**, *369*, 471−473.
(249) Thrane, L.; Jacobsen, R. H.; Jepsen, P. U.; Keiding, S. R. *Chem. Phys. Lett.* **1995**, *240*, 330−333.
(250) Kindt, J. T.; Schmuttenmaer, C. A. *J. Phys. Chem.* **1996**, *100*, 10373−10379.
(251) Rønne, C.; Thrane, L.; Åstrand, P.-O.; Wallqvist, A.; Mikkelsen, K. V.; Keiding, S. R. *J. Chem. Phys.* **1997**, *107*, 5319−5331.
(252) Rønne, C.; Åstrand, P.-O.; Keiding, S. R. *Phys. Rev. Lett.* **1999**, *82*, 2888−2891.
(253) Woutersen, S.; Emmerichs, U.; Bakker, H. J. *Science* **1997**, *278*, 658−660.
(254) Paciaroni, A.; Bizzarri, A. R.; Cannistraro, S. *Phys. Rev. E* **1998**, *57*, R6277−R6280.
(255) Paciaroni, A.; Bizzarri, A. R.; Cannistraro, S. *Phys. Rev. E* **1999**, *60*, R2476−R2479.
(256) Angell, C. A. *Nature* **1988**, *331*, 206−207.
(257) Tanaka, H. *Nature* **1996**, *380*, 328−330.
(258) Tanaka, H. *Phys. Rev. Lett.* **1998**, *80*, 113−116.
(259) Carignano, M. A.; Karlström, G.; Linse, P. *J. Phys. Chem. B* **1997**, *101*, 1142.
(260) Cristinziano, P.; Lelj, F.; Amodeo, P.; Barone, V. *Chem. Phys. Lett.* **1987**, *140*, 401−405.
(261) Cristinziano, P.; Lelj, F.; Amodeo, P.; Barone, G.; Barone, V. *J. Chem. Soc., Faraday Trans. 1* **1989**, *85*, 621−632.
(262) Boek, E. S.; Briels, W. J. *J. Chem. Phys.* **1993**, *98*, 1422−1427.
(263) Finney, J. L.; Turner, J. *Electrochim. Acta* **1988**, *33*, 1183−1190.
(264) Finney, J. L.; Soper, A. K.; Turner, J. *Physica B* **1989**, *156*−*157*, 151−153.
(265) Hermida-Ramón, J. M.; Rios, M. A. *J. Phys. Chem. A* **1998**, *102*, 10818.
(266) Cabaleiro-Lago, E. M.; Ríos, M. A. *Chem. Phys.* **1998**, *236*, 235−242.
(267) Price, S. L.; Faerman, C. H.; Murray, C. W. *J. Comput. Chem.* **1991**, *12*, 1187.
(268) Blaney, J. M.; Weiner, P. K.; Dearing, A.; Kollman, P. A.; Jorgensen, E.; Oatley, S. J.; Burridge, J. M.; Blake, C. C. F. *J. Am. Chem. Soc.* **1982**, *104*, 6424.
(269) Koch, U.; Popelier, P. L. A.; Stone, A. J. *Chem. Phys. Lett.* **1995**, *238*, 253.
(270) Strasburger, K.; Sokalski, W. A. *Chem. Phys. Lett.* **1994**, *221*, 129.
(271) Jorgensen, W. L.; Buckner, J. K. *J. Chem. Phys.* **1987**, *91*, 6083.
(272) Hooft, R. W. W.; van Eijck, B. P.; Kroon, J. *J. Chem. Phys.* **1992**, *97*, 6690.
(273) Bedrov, D.; Borodin, O.; Smith, G. D. *J. Phys. Chem. B* **1998**, *102*, 5683.
(274) Bedrov, D.; Smith, G. D. *J. Chem. Phys.* **1998**, *109*, 8118.
(275) Jaffe, R. L.; Smith, G. D.; Yoon, D. Y. *J. Phys. Chem.* **1993**, *97*, 12745.
(276) Mikkelsen, K. V.; Ågren, H.; Jensen, H. J. A.; Helgaker, T. *J. Chem. Phys.* **1988**, *89*, 3086−3095.
(277) Mikkelsen, K. V.; Jørgensen, P.; Ruud, K.; Helgaker, T. *J. Chem. Phys.* **1997**, *106*, 1170−1180.
(278) Cramer, C. J.; Truhlar, D. G. *Chem. Rev.* **1999**, *99*, 2161−2200.
(279) Chesnut, D. B.; Rusiloski, B. E. *J. Mol. Struct. (THEOCHEM)* **1994**, *314*, 19−30.
(280) Malkin, V. G.; Malkina, O. L.; Steinebrunner, G.; Huber, H. *Chem. Eur. J.* **1996**, *2*, 452.
(281) McDowell, S. A. C.; Le Sueur, C. R.; Buckingham, A. D.; Stone, A. J. *Mol. Phys.* **1992**, *77*, 823−835.
(282) Nymand, T. M.; Åstrand, P.-O.; Mikkelsen, K. V. *J. Phys. Chem. B* **1997**, *101*, 4105−4110.
(283) Buckingham, A. D.; Tantirungrotechai, Y. *Mol. Phys.* **1999**, *96*, 1217−1224.
(284) Buckingham, A. D.; Tantirungrotechai, Y. *Mol. Phys.* **1999**, *96*, 1225−1229.
(285) McConnel, H. M. *J. Chem. Phys.* **1957**, *27*, 226−229.
(286) Stephen, M. J. *Mol. Phys.* **1958**, *1*, 223−232.
(287) Buckingham, A. D.; Schaefer, T.; Schneider, W. G. *J. Chem. Phys.* **1960**, *32*, 1227−1233.
(288) Buckingham, A. D. *Canad. J. Chem.* **1960**, *38*, 300−307.
(289) Batchelor, J. G. *J. Am. Chem. Soc.* **1975**, *97*, 3410−3415.
(290) Augspurger, J. D.; Dykstra, C. E.; Oldfield, E. *J. Am. Chem. Soc.* **1991**, *113*, 2447−2451.
(291) Augspurger, J.; Pearson, J. G.; Oldfield, E.; Dykstra, C. E.; Park, K. D.; Schwartz, D. *J. Magn. Res.* **1992**, *100*, 342−357.
(292) Augspurger, J. D.; Dykstra, C. E. *J. Am. Chem. Soc.* **1993**, *115*, 12016−12019.
(293) Nymand, T. M.; Åstrand, P.-O. *J. Chem. Phys.* **1997**, *106*, 8332−8338.
(294) Nymand, T. M.; Åstrand, P.-O. *J. Phys. Chem. A* **1997**, *101*, 10039−10044.
(295) Roos, B. O. *Adv. Chem. Phys.* **1987**, *69*, 399−445.

CR9900477